

TIME-DEPENDENT DISK MODELS FOR THE MICROQUASAR GRS 1915+105

SERGEI NAYAKSHIN^{1,2,3}, SAUL RAPPAPORT⁴, AND FULVIO MELIA^{5,6}*Draft version June 16, 2021*

ABSTRACT

During the past two years, the galactic black hole microquasar GRS 1915+105 has exhibited a bewildering diversity of large amplitude, chaotic variability in X-rays. Although it is generally accepted that the variability in this source results from an accretion disk instability, the exact nature of the instability remains unknown. Here we investigate different accretion disk models and viscosity prescriptions in order to provide a basic explanation for the exotic temporal behavior in GRS 1915+105.

We discuss a range of possible accretion flow geometries. Based on the fact that the overall cycle times are very much longer than the rise/fall time scales in GRS 1915, we rule out the geometry of advection dominated accretion flow (ADAF) or a hot quasi-spherical region plus a cold outer disk for this source. A cold disk extending down to the last inner stable orbit plus a hot corona above it, on the other hand, is allowed.

We thus concentrate on geometrically thin (though not necessarily standard) Shakura-Sunyaev type disks (Shakura & Sunyaev 1973; hereafter SS73). We argue that X-ray observations clearly require a quasi-stable accretion disk solution at high accretion rates where radiation pressure begins to dominate, which excludes the standard α -viscosity prescription. To remedy this deficiency, we have therefore devised a modified viscosity law that has a quasi-stable upper branch, and we have developed a code to solve the time-dependent equations to study such an accretion disk. Via numerical simulations, we show that the model does account for several gross observational features of GRS 1915+105, including its overall cyclic behavior on time scales of $\sim 100 - 1000$ s. On the other hand, the rise/fall time scales are not short enough, no rapid oscillations on time scales $\lesssim 10$ s emerge naturally from the model, and the computed cycle-time dependence on the average luminosity is stronger than is found in GRS 1915+105.

We then consider, and numerically test, several effects as a possible explanation for the residual disagreement between the model and the observations. A hot corona with the energy input rate being a function of the local cold disk state and a radius-dependent α -parameter do *not* appear to be promising in this regard. However, a more elaborate model that includes the cold disk, a corona, and plasma ejections from the inner disk region allows us to reproduce several additional observed features of GRS 1915+105. We conclude that the most likely structure of the accretion flow in this source is that of a cold disk with a modified viscosity prescription, plus a corona that accounts for much of the X-ray emission, and unsteady plasma ejections that occur when the luminosity of the source is high. The disk is geometrically thin due to the fact that most of the accretion power is drained by the corona and the jet.

Subject headings: accretion disks, black holes, binary X-ray sources, microquasars

1. INTRODUCTION

Compact X-ray sources exhibit a wide range of temporal variabilities (from milliseconds to years). Perhaps none of these is as exotic and diverse as the X-ray temporal variability observed from the black hole microquasar GRS 1915+105 (Castro-Tirado, Brandt, & Lund 1992; Greiner, Morgan, & Remillard 1996; Morgan, Remillard & Greiner 1997; Munoz, Morgan & Remillard 1999). This object is one of two known Galactic X-ray sources that exhibit superluminal radio jets (Mirabel & Rodrigues 1994). The combination of relativistic constraints and radio measurements at HI indicate that the source lies behind the Sagittarius arm at a distance of 12.5 ± 1.5 kpc (Mirabel & Rodrigues 1994). Interstellar extinction limits optical/IR

studies to weak detections at wavelengths less than 1 micron (Mirabel et al. 1997). The source is suspected to be a black hole binary because of its spectral and temporal similarities with the other Galactic X-ray source with superluminal radio jets, GRO J1655-40 (Zhang et al 1994), which has a binary mass function indicative of a black hole system (Bailyn et al. 1995). Estimates for the mass of the compact object in GRS 1915+105 range from 7 to $33 M_{\odot}$. Even with the uncertainty in distance, its peak X-ray luminosity is unusually high, i.e., $\gtrsim 10^{39}$ ergs/sec, which is around the Eddington luminosity for a $\sim 7 M_{\odot}$ object.

In spite of several attempts it has proven especially illusive to interpret the X-ray light curves of GRS1915. It is not yet clear that even the basic time scales exhibited by the variability have been successfully explained. Belloni et

¹Physics Department, The University of Arizona, Tucson, AZ 85721.²LHEA, GSFC/NASA, Code 661, Greenbelt, MD, 20771.³National Research Council Associate.⁴Physics Department and Center for Space Research, MIT, Cambridge, MA 02139.⁵Physics Department and Steward Observatory, The University of Arizona, Tucson, AZ 85721.⁶Sir Thomas Lyle Fellow.

al. (1997a,b) accounted for the observations with an empirical model in which the inner disk region “disappears” in the low count rate state, and is then replenished on a viscous time scale. The parameters of their model are: the inner disk radius, R_{in} ; the corresponding effective temperature of the disk T_{in} , and an ad-hoc non-thermal power law (which is possibly produced in the disk corona). Although no detailed physical model for the instability was given, very interesting patterns of behavior for R_{in} and T_{in} , as well as several other observables, were deduced from the data, and the Shakura-Sunyaev viscosity parameter was found to be unexpectedly low (which may mean that the standard viscosity prescription is invalid for this source). The rather small values of R_{in} found by these authors can be used to discriminate between different models of the accretion flow in GRS 1915 (see Appendix and §6).

Abramowicz, Chen & Taam (1995) suggested a model for the low frequency quasi-periodic oscillations (QPO) observed in selected X-ray binaries, in which a corona above the *standard accretion* disk leads to a mild oscillatory behavior. With some modifications, this model could reasonably be expected to account for at least some of the temporal variability in GRS 1915+105 as well (Taam, Chen & Swank 1997). However, it appears to us that the analysis of Abramowicz et al. (1995) and Taam et al. (1997) contains an error in the heating/cooling equation for the disk which, when corrected, constrains their model to have the same stability characteristics as a standard Shakura-Sunyaev disk, and is therefore unlikely to explain the GRS 1915+105 observations (see Appendix A).

We show more generally in Appendix A that neither a hot central region, nor an advection-dominated flow, nor a “slim” accretion disk are compatible with the observations of GRS 1915+105. (“Slim” accretion disk theory was developed in the most detail by Abramowicz et al. 1988; it is similar to a standard thin Shakura-Sunyaev disk, except for the energy equation, which incorporates the radial advection of energy into the black hole.) In this paper, we attempt to undertake a more systematic study of the variability patterns in GRS 1915+105 within the context of the “cold disk+hot corona” picture. In §2 we present a general discussion that will guide us in our selection of a novel (though somewhat ad-hoc) prescription for the viscosity in cases where the radiation pressure is substantial (§3.2). The details of our numerical algorithm to solve the time-dependent disk equations with the use of this new viscosity prescription are given in §3.1.

In §4, we present the results of our time-dependent disk calculations. The calculated light curves are found to agree qualitatively with many observational features of GRS 1915+105. In particular, the characteristic cycle times and duty cycles are in reasonable agreement with the observations. Moreover, the trend in the cycle time with the average accretion rate, \dot{m} has the correct sense. However, there are important disagreements as well. We therefore introduce a more elaborate model in §5, where, in accordance with the observations (e.g., Mirabel & Rodriguez 1994), the inner disk is allowed to expel some of its energy in the form of a non-steady jet. We assume that the ejected energy is not observed in X-rays, but rather that it ultimately produces radio emission. We show that this more elaborate model agrees with the GRS 1915+105 observations much better, perhaps indicating that we are

finally developing a zeroth order understanding of the geometry and the most important processes in this enigmatic source. In §6 we discuss our results in the light of the earlier work on GRS 1915, and in §7 we summarize our conclusions.

2. LIMIT CYCLE BEHAVIOR IN GRS 1915+105

Figure 1 shows four examples of typical X-ray light curves from GRS 1915 obtained with the RXTE satellite (see, e.g., Morgan, Remillard, & Greiner 1997). It appears that the source undergoes a limit-cycle type of instability; the cycle times in panels (a) – (d) are ~ 2400 , 60 , 1200 , and 800 sec, respectively. Within the cycles shown in panels (c) and (d) there appear yet other quasi-regular oscillations of still shorter time scale. The shortest time scale over which a substantial change in the X-ray flux occurs is ~ 5 sec. We will associate the longer cycles with the viscous time scales of the inner accretion disk, whereas the more rapid behavior will be related to the thermal time scale. The X-ray spectrum of GRS 1915+105 varies systematically with X-ray intensity; usually the spectral hardness is strongly correlated (or anti-correlated) with intensity (e.g., Belloni et al. 1997a,b; Taam et al. 1997; Munoz et al. 1999). More specifically, the spectrum is typically found to be composed of a multi-temperature disk component, hereafter the “thermal component”, and a power-law component with a varying spectral index. Finally, the source exhibits a wide range of QPOs with central frequencies in the range of 0.01 – 10 Hz. The amplitude and frequency of the QPOs appear to be strongly correlated with the spectral state of GRS 1915+105 (Chen et al. 1997; Munoz et al. 1999).

The idea of using a modified viscosity law to test time-dependent phenomena in accretion disks around black holes is not new (e.g., Taam & Lin 1984; Chen & Taam 1994; and further references below in this section). But let us examine in global terms how the various disk configurations relate to the behavior of GRS 1915+105 in particular. In geometrically thin disks the advection of energy is not important. The viscous time scale is much longer than both the thermal and hydrostatic time scales (see Frank et al. 1992), unless $\alpha \sim 1$ which is unlikely for this source (Belloni et al. 1997b). In this context, then, the equations for vertical hydrostatic equilibrium and energy balance between viscous heating and radiative losses should be valid.

It is customary and instructive to plot the disk effective temperature T_{eff} versus the column density Σ to investigate the stability properties of disks. In the one zone limit, the equation for hydrostatic equilibrium in the vertical direction is

$$P_{\text{tot}} \equiv P_{\text{gas}} + P_{\text{rad}} = \frac{GM\Sigma H}{2R^3}, \quad (1)$$

where M is the mass of the black hole, H is the scale height and R is the radial distance from the central object. The gas pressure is given by $P_{\text{gas}} = 2\rho m_p^{-1}kT$ (for hydrogen rich material), where T is the mid-plane temperature, m_p is the proton mass, and the radiation pressure is $P_{\text{rad}} = aT^4/3$. The energy balance equation is given by

$$F_{\text{rad}} \simeq \frac{cP_{\text{rad}}}{\tau} = \frac{3}{2}\sigma_{r\phi} \Omega H, \quad (2)$$

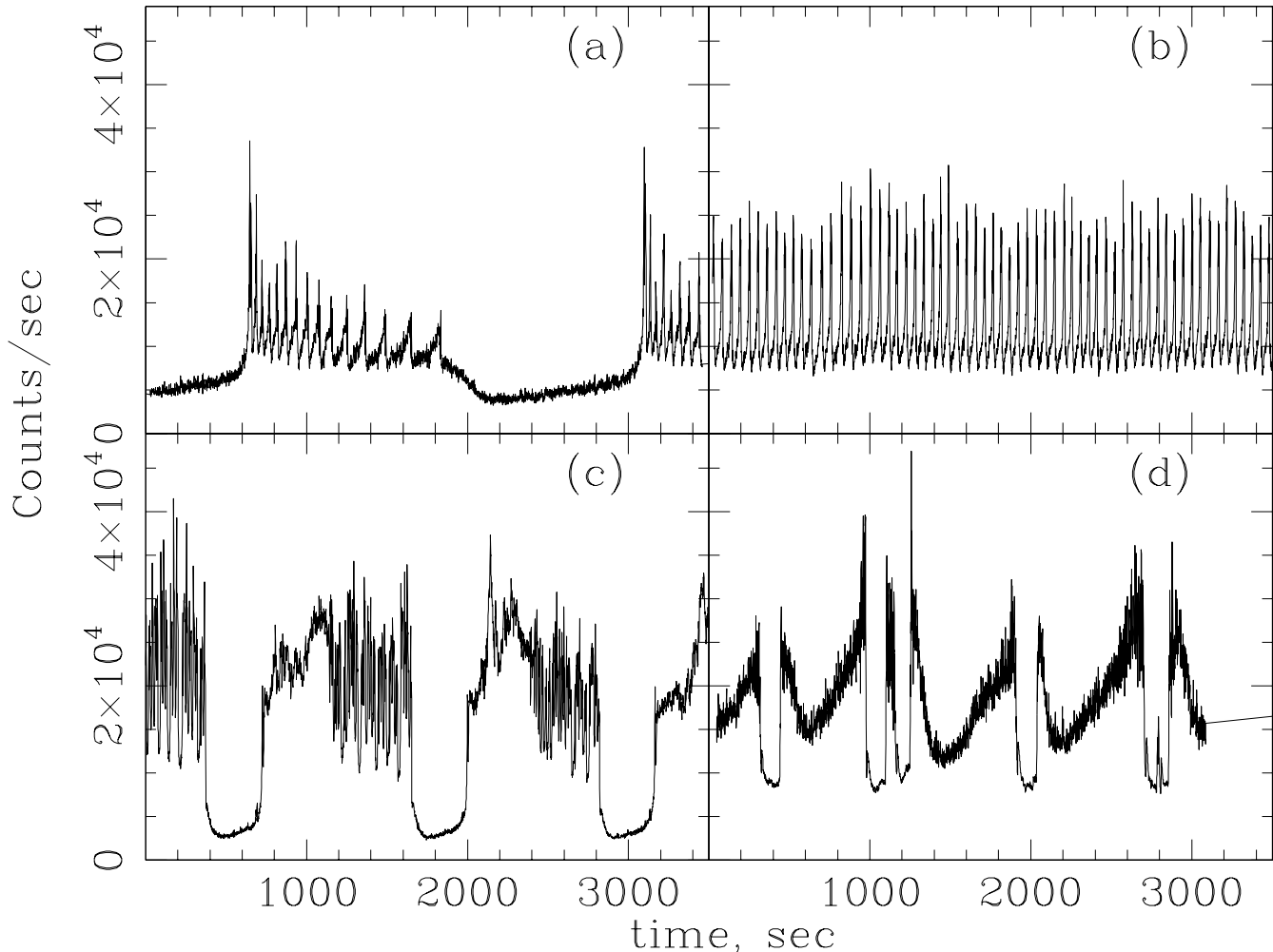


FIG. 1.— Selected segments of the X-ray light curve of GRS 1915+105, demonstrating the broad range of variability patterns in this unusual source. The data were obtained from the public archive of the Rossi X-ray Timing Explorer (RXTE).

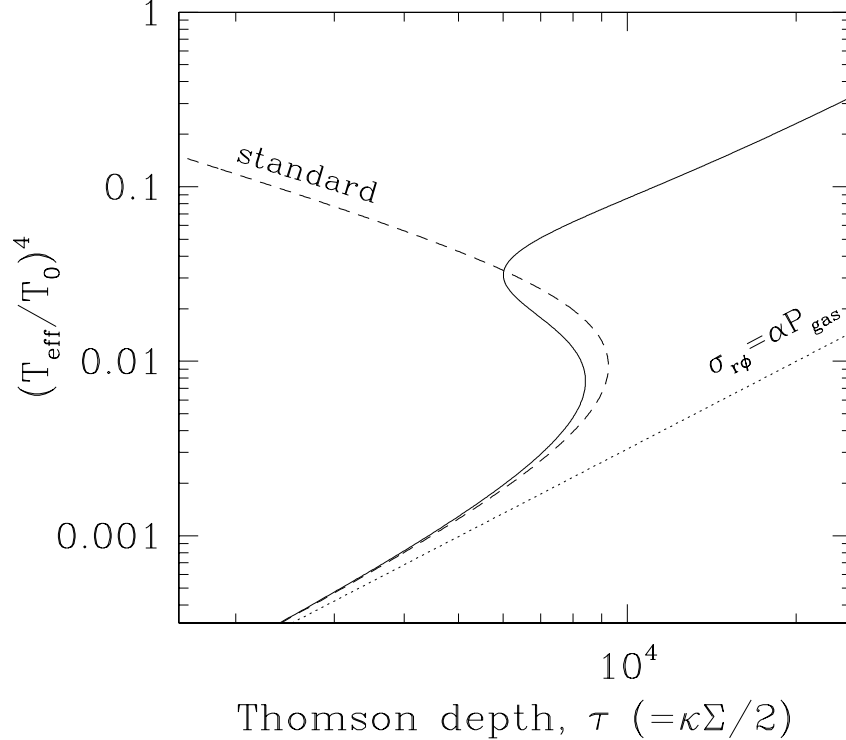


FIG. 2.— Effective temperature versus the Thomson optical depth at a fixed radial distance R_0 for accretion disks with the standard (dashed curve), Lightman-Eardley (dotted), and our modified viscosity prescription (solid curve). T_0 is defined as the effective temperature of the disk at R_0 for the case where the disk radiates at the Eddington luminosity (e.g., $\dot{m} = 1$). The lower bend in the S-curve occurs due to the radiation pressure starting to dominate within the disk, while the higher bend is introduced by requiring the viscosity law to follow the Lightman-Eardley form above some value for $P_{\text{rad}}/P_{\text{gas}}$.

where F_{rad} is the vertical radiation flux, τ is the optical depth of the disk, $\tau \equiv \kappa\Sigma/2$, and κ is the radiative opacity (assumed to be dominated by electron scattering opacity), $\sigma_{r\phi}$ is the stress tensor (see, e.g., Shapiro & Teukolsky, §14.5), and Ω is the Keplerian angular frequency. As we said earlier, in the standard Shakura-Sunyaev formulation, the stress tensor is proportional to the total pressure,

$$\sigma_{r\phi} = \alpha P_{\text{tot}}. \quad (3)$$

We can now combine Equations (1) – (3) to eliminate the variable H and thereby derive an expression to generate the $T_{\text{eff}}-\Sigma$ curve for any given viscosity. In Figure (2) we show several illustrative $T_{\text{eff}}-\Sigma$ curves to help motivate our selection of α . The dashed curve represents the track that the standard Shakura-Sunyaev theory with $\alpha = \text{const}$ produces. Such a model is thermally and viscously unstable when the slope of the $T_{\text{eff}}-\Sigma$ curve becomes negative (e.g., Frank et al. 1992), which might be a desirable result in the view of the instabilities observed in GRS 1915+105. However, the observed light curves require a quasi-stable accretion mode for the high-luminosity state as well, which is *not predicted* by the standard theory (see also the end of App. B). This suggestion (already discussed by Belloni et al. 1997a,b and Taam et al. 1997) is motivated by the fact that in some cases the upper luminosity state of the source lasts even longer than the low state, which is presumably the stable gas-pressure-dominated branch. A $T_{\text{eff}}-\Sigma$ relation that has a stable high-luminosity state is shown in Figure (2, solid curve). It has the characteristic “S-shape”, familiar from the studies of the thermal ionization instability in accretion disks (e.g., Meyer & Meyer-Hofmeister

1981, Bath & Pringle 1982, Cannizzo, Chen & Livio 1995, and Frank et al. 1992, §5.8) or from studies of radiation-pressure driven instabilities by, e.g., Taam & Lin (1984) and Chen & Taam (1994). It is well known that parts of an S-curve that have a negative slope are unstable. In short, when the $T_{\text{eff}}-\Sigma$ relation produces an S-curve, the unstable region of the disk oscillates between the two stable branches of the solution, which gives rise to the high and low luminosity states.

So far, we have not considered flows where advection is important. As ADAFs (Advection Dominated Accretion Flows) will be discussed in §A.1, here we concentrate on the slim accretion disks (Abramowicz et al. 1988). These flows have a stable high \dot{m} solution even with the standard viscosity prescription due to the additional cooling (energy transport) via advection. However, the S-curves produced by these models have the upper stable branch for $\dot{m} \gtrsim 1$ only (see, e.g., see Fig. 2 in Chen & Taam 1993). In other words, if one were to position the upper stable branch of the slim accretion disks on our Figure (2), then it would look similar to the corresponding stable branch of the solid curve in the figure, except that it would be positioned higher by a factor of about 100 (at a given Σ). Thus, if one assumes that an unstable part of the disk makes a transition from the lower bend in the S-curve upwards to the stable branch, and that Σ remains approximately constant during this process, then the accretion rate in the inner disk must increase by as much a factor of a few hundred to a thousand to reach the stable advective regime.

While this may not be a problem in terms of the lumi-

nosity output, since most of the energy is advected inwards and the luminosity of the disk saturates at $L \simeq L_{\text{Edd}}$ (see Fig. 1 in Szuszkiewicz, Malkan & Abramowicz 1996), the light curves produced will always be very spiky and the duty cycle of the high state is always much smaller than the values of ~ 0.5 that are often seen in GRS 1915+105. The physical cause of the spiky behavior is the vast difference between the accretion rates in the high and low states. As we will discuss later in §4, an outburst starts because “too much” mass (column density Σ) has been accumulated above the maximum possible stable value of Σ_{max} (i.e., Σ at the lower bend of the S-curve in Figure 2). If the high stable state accretion rate is very much larger than the low state accretion rate, it then takes only a very short time in the high state to remove this excess mass from the inner disk. In other words, it would not be possible to maintain mass conservation if the accretion rate persisted at the high state for very long. This is indeed seen from the temperature curves computed for slim disks by Szuszkiewicz & Miller (1998, see their Figures 7–9). Therefore, we believe that slim disks are not likely to adequately account for the behavior of GRS 1915+105, at least not if one seeks a theory capable of explaining all of the variability in this source.

3. THE BASIC MODEL

3.1. Time-Dependent Equations For Disk-Corona Models

The geometry in our unstable disk model is that of a standard Shakura-Sunyaev configuration (except for the viscosity law) overlayed with a hot corona. Here we describe the set of equations that we use to follow the temporal evolution of this disk; these equations are applicable to any local viscosity law. A discussion of the viscosity itself is deferred until §3.2. The standard Euler equations for conservation of mass and angular momentum in the disk (see, e.g., Frank et al. 1992) can be combined in the usual way to yield the equation describing the evolution of the surface density:

$$\frac{\partial \Sigma}{\partial t} = \frac{3}{R} \frac{\partial}{\partial R} \left\{ R^{1/2} \frac{\partial}{\partial R} [\nu \Sigma R^{1/2}] \right\}, \quad (4)$$

where all of the variables, except for ν , were defined in the previous section. Here ν is the viscosity that is related to α by $\alpha P_{\text{tot}} = \frac{3}{2} \nu \Omega \rho$.

The time-dependent energy equation includes the heating and cooling terms of Equation (2), but must also be able to take into account large radial gradients of temperature, and therefore includes a number of additional terms. The form of the energy equation that we use follows the formalism of Abramowicz et al. (1995) with some modifications, and is given by

$$\begin{aligned} P_{\text{tot}} H \frac{4-3\beta}{\Gamma_3-1} & \left[\left(\frac{\partial \ln T}{\partial t} + v_R \frac{\partial \ln T}{\partial R} \right) \right. \\ & \left. - (\Gamma_3-1) \left(\frac{\partial \ln \Sigma}{\partial t} + v_R \frac{\partial \ln \Sigma}{\partial R} - \frac{\partial H}{\partial t} \right) \right] \\ & = F^+ - F^- - \frac{2}{R} \frac{\partial (R F_R H)}{\partial R} + J, \quad (5) \end{aligned}$$

where $\beta = 1/(1+\xi)$, $\xi = P_{\text{rad}}/P_{\text{gas}}$ is the ratio of the radiation to the gas pressure, γ is the ratio of specific heats ($\gamma = 5/3$) and Γ_3 is given in Abramowicz et al. (1995). The radial velocity v_R is given by the standard expression (Eq. 5.7 of Frank et al. 1992):

$$v_R = -\frac{3}{\Sigma R^{1/2}} \frac{\partial}{\partial R} [\nu \Sigma R^{1/2}]. \quad (6)$$

The terms on the left hand side of Equation (5) represent the full time derivative (e.g., $\partial/\partial t + v_R \partial/\partial R$) of the gas entropy, while the terms on the right are the viscous heating, the energy flux in the vertical direction, the diffusion of radiation in the radial direction, and the viscous diffusion of thermal energy. Following Cannizzo (1993; and references cited therein), we take $J = 2c_p \nu (\Sigma/R) [\partial(R \partial T / \partial R) / \partial R]$ to be the radial energy flux carried by viscous thermal diffusion, where c_p is the specific heat at constant pressure. F^+ is the accretion disk heating rate per unit area, and is given by

$$F^+ = \frac{9}{4} \nu \Sigma R \Omega_K^2. \quad (7)$$

The radiation flux in the radial direction is

$$F_R = -2 \frac{c P_{\text{rad}}}{\tau_T} H \frac{\partial \ln T}{\partial R}. \quad (8)$$

The overall cooling rate (larger than simply that from radiative diffusion) in the vertical direction is given by

$$F^- = \frac{c P_{\text{rad}}}{\tau_T} (1-f)^{-1}, \quad (9)$$

where $0 \leq f < 1$ is the fraction of the power that is transferred to the disk surface by mechanisms other than the usual radiation diffusion (cf. Abramowicz et al. 1995, Svensson & Zdziarski 1994). Equations (7) and (9) differ from those used by Abramowicz et al. (1995) for reasons that are detailed in Appendix B. We note that in the most general sense, the quantity $(1-f)^{-1}$ should be thought of as a factor correcting the vertical energy transport in the standard accretion disk theory. In our formulation of the problem, it is computationally irrelevant whether this fraction of energy is deposited in the corona and radiated as a non-thermal power-law component, or it contributes to the blackbody disk flux, since we are concerned only with the bolometric luminosity of the disk for now. The latter case could be realized if this additional energy transport were to deposit its energy just below the photosphere of the disk. Of course, if our model produces light curves that are in reasonable agreement with those of GRS 1915+105, then a future study, one that would carefully delineate the different spectral components, will be warranted.

Equations (4) and (5), together with the equation of hydrostatic equilibrium (1), yield a closed set of coupled, time-dependent equations for evolving the variables T and Σ . For solving these equations we employ a simple explicit scheme with a variable time step. The time step is chosen to be always a fraction of the smallest thermal time scale in the disk (i.e., in its inner part). We also use a fixed grid in R . The spacing is uniform in $R^{1/2}$, and we take 100 to 300 radial bins. We will often refer to the radial coordinate in a dimensionless form, i.e., $r \equiv R/R_g$, where $R_g = 2GM/c^2$

is the Schwarzschild radius. The outer boundary of the disk is chosen at a large radius, $r_{\max} \sim$ few hundred to a thousand, such that the disk at $r \gtrsim r_{\max}/3$ is always gas-pressure dominated. Thus, the outer boundary conditions are given by $T = T_{\text{ss}}$ and $\Sigma = \Sigma_{\text{ss}}$ for $r = r_{\max}$, where T_{ss} and Σ_{ss} are the temperature and the column density in the Shakura-Sunyaev formulation at that radius for the given f , \dot{m} and $\alpha = \alpha_0$, where α_0 is the viscosity parameter for a gas-dominated disk (see below). The inner boundary of the disk is fixed at $r = 3$, and the boundary conditions there are $T = 0$ and $\Sigma = 0$.

3.2. Modified Viscosity Law

In this section we present our modified viscosity law that we anticipate will account for the unstable behavior of GRS 1915+105. The Shakura-Sunyaev viscosity prescription postulates that the viscous stress tensor $\sigma_{r\phi}$ is given by Equation (3), where the parameter α is defined as

$$\alpha \simeq (v_t l_t / c_s H) + (B^2 / 4\pi P_{\text{tot}}), \quad (10)$$

and where v_t and l_t are the turbulent eddy velocity and scale-length, respectively, c_s is the sound speed, and $B^2 / 4\pi$ is the volume averaged magnetic field energy density. Obviously, this approach is useful only when α remains approximately constant, i.e., independent of the local thermodynamic variables in the disk, which is probably the case in a number of situations. However, whenever the physical state of the accreting gas changes considerably, it is hard to see why α would not change. One confirmation of this is the well-known thermal (ionization) instability of accretion disks in dwarf nova systems (e.g., Meyer & Meyer-Hofmeister 1981; Bath & Pringle 1982; Cannizzo, Chen & Livio 1995; and Frank et al. 1992; §5.8). It has been shown in this case that the α -parameter needs to be larger on the hot stable branch than it is on the low branch of the solution. Some more recent work suggests that, in addition, α should have a power-law dependence on (H/R) , e.g., $\alpha \propto (H/R)^{3/2}$, in order to explain the observed exponential luminosity decline of the dwarf nova outbursts (Cannizzo et al. 1995; Vishniac & Wheeler 1996).

Further, based on theoretical considerations, different authors have adopted several variants on the prescription for $\sigma_{r\phi}$ when $P_{\text{rad}} \geq P_{\text{gas}}$. For example, Lightman & Eardley (1974; hereafter LE74), and Stella & Rosner (1984; hereafter SR84) suggested that

$$\sigma_{r\phi} = \alpha_0 P_{\text{gas}}, \quad (11)$$

where α_0 is a constant. Their physical reasoning was based on the expectation that chaotic magnetic fields should be limited by the gas pressure only. In addition, Sakimoto & Coronitti (1989; hereafter SC89) showed that even if one assumes that magnetic fields are effectively generated by radiation-dominated disks, magnetic buoyancy quickly expels these fields from the disks. Since the disk viscosity may be produced to a large extent by magnetic fields, this result implies that the α -parameter must decrease when the radiation pressure becomes dominant. An attractive feature of this viscosity prescription (Eq. 11) is the fact that it is stable even when $P_{\text{rad}} \geq P_{\text{gas}}$, as indicated by the positive slope generated by this model for the track in

$T_{\text{eff}}-\Sigma$ parameter space (see the dotted curve in Fig. 2). At the same time, however, this viscosity prescription (to which we will refer as the Lightman-Eardley prescription) has no unstable region at all, and thus fails to reproduce the unstable behavior observed in GRS 1915+105.

Of course, the conclusions of LE74, SR84 and SC89 should be regarded as qualitative, at best, since it is not yet feasible to describe the turbulence and magnetic fields immersed in a radiation-dominated fluid in a quantitative and model-independent way. In this paper, we adopt the view that it may still be possible to couple the radiation to the particles through collisions and thereby allow the radiation pressure to contribute to the viscosity when $P_{\text{rad}}/P_{\text{gas}}$ is not too great. For example, SR84 argued that the energy density in the chaotic magnetic fields cannot exceed the particle energy density, since it is the latter that generates the magnetic fields in the first place. However, as long as $P_{\text{rad}}/P_{\text{gas}} < \alpha^{-1}$, the magnetic field pressure does not exceed the gas pressure (because then $B^2/8\pi \sim \alpha P_{\text{rad}} < P_{\text{gas}}$), so that the SR84 arguments are superfluous.

To cast our suggestion into a mathematical form, we have adopted a viscosity prescription intermediate between those of Shakura-Sunyaev and Lightman-Eardley. Our viscosity law is proportional to the total pressure for small to moderate values of $\xi = P_{\text{rad}}/P_{\text{gas}}$, while for large values of ξ , it becomes proportional to the gas pressure. We have devised the following simple formula for the viscosity prescription that smoothly joins these two limits, such that α is given by

$$\alpha = \alpha_0 \frac{1 + \xi/\xi_0}{1 + (\xi/\xi_0)^2}, \quad (12)$$

where ξ_0 is an adjustable parameter. The S-curve plotted in Figure (2) was generated using this viscosity prescription with $\xi_0 = 8$.

4. RESULTS

4.1. Accretion Disk Evolution Through One Cycle

There are essentially 5 free parameters of the model that need to be specified and/or systematically varied to ascertain the sensitivity of the results to their value: (i) the black hole mass, M , (ii) the average accretion rate, \dot{m} , (iii) the viscosity parameter, α_0 , for the gas-dominated region, (iv) ξ_0 , the critical ratio $P_{\text{rad}}/P_{\text{gas}}$, and (v) f , the fraction of the luminosity transported vertically by mechanisms other than radiative diffusion. We adopt a mass of $10 M_{\odot}$, which is typical of the measured masses of galactic black hole candidates in binary systems (see, e.g., Barret et al. 1996). For purposes of illustration, we chose a value of α_0 equal to 0.01, since it leads to viscous time scales comparable to those observed. Similarly, we selected a value of $\xi_0 = 8$, in part because it produces a reasonable S-curve. However, we checked a range of other values as well (from $\xi_0 = 3$ to $\xi_0 = 20$), and found that $\xi = 8$ reproduces the GRS 1915+105 observations most closely.

We present a computed light curve and variations of the disk parameters through one complete cycle in Figures (3) and (4), respectively, for one set of illustrative parameters: $\dot{m} = 0.05$ and $f = 0$. In Figure (4), panels (a), (b), (c) and (d) show the evolution of the disk effective temperature T_{eff} , the ratio of radiation to gas pressure (ξ), the disk

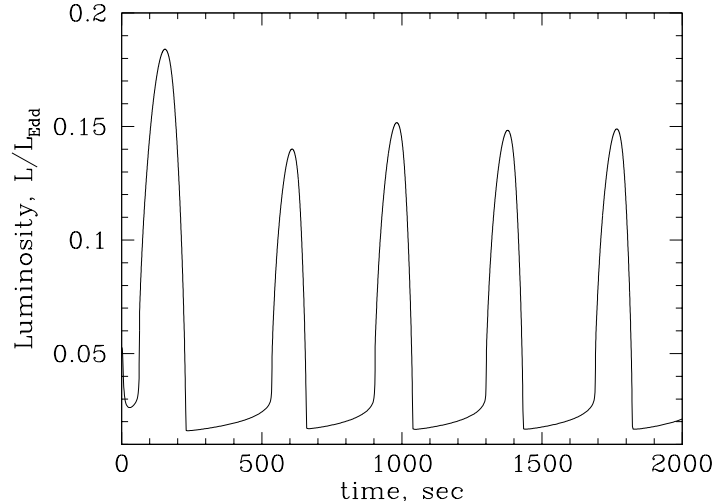


FIG. 3.— The light curve for an unstable disk with parameters $f = 0$ and $\dot{m} = 0.05$.

Thomson optical depth τ and the radial flow velocity v_r . Note that since we are currently concerned only with the luminosity integrated over all photon energies, we define T_{eff} to include the emissivity from *both* the corona and the disk, i.e., $\sigma_B T_{\text{eff}}^4 \equiv F^-$, where F^- is given by Equation (9). In each panel, the series of curves are for temporal increments of ~ 7.5 sec.

The curve with the smallest luminosity L (where $L = \int 2\pi R \sigma_B T_{\text{eff}}^4 dR$) in the upper left panel of Figure (4) corresponds to the state of the disk right after the end of an outburst. An outburst starts in the innermost region of the disk, when a few zones at the smallest radii quickly make a transition to the upper stable branch of the solution (high state). Although this is not obvious from Fig. (4), the viscosity of the high state is larger than it is in the low state, because $\nu = \alpha c_s H$, and so even though α decreases, the increase in c_s and H leads to a larger ν . The larger viscosity allows the gas to dispose of its angular momentum faster, thus allowing a faster inflow of the gas into the black hole. Because of angular momentum conservation, the angular momentum of the gas that plummets into the black hole is transferred to larger R , where it produces an excess of angular momentum, and thus some matter actually flows to larger R , which is seen in panel (d) of Figure (4) as positive spikes in the radial velocity distribution. A heating wave is initiated and propagates from the inner disk to larger R (Fig. 4a). This wave is often referred to as either a ‘density wave’ or a ‘transition wave’. As the wave propagates outward, the material on the inside of the wave becomes hot and shifts into the high viscosity state. It then rapidly loses its angular momentum and is transferred into the innermost disk, where the material continuously plummets into the hole. Since the innermost stable region is a “bottle-neck” for the accreting gas, some material builds up there, which explains the bump in Σ in that region as seen in Figure (4c) during the outburst.

When the density wave reaches $r \sim 100$, the instability saturates, since the disk in that region is always gas-pressure dominated (for the chosen \dot{m} and f). As the density wave dies away, the outermost unstable regions are cleared of the excess mass and cool down. They are now in the low viscosity state, and thus the rate of mass inflow

in the innermost region of the disk drops. An inward propagating cooling wave is initiated and the outburst dies out as the last excess mass in the innermost disk sinks into the hole. Finally, a new cycle begins with the accumulation of new excess mass (since the local accretion rate is smaller than the average rate).

4.2. Light curves

We now systematically explore the disk behavior with the new viscosity prescription, in order to eventually compare the results with the gross temporal behavior of GRS 1915+105. We adopted an energy transport fraction $f = 0.9$. As with the other parameters, we also tested a wide range of values of f , and found that $f = 0.9$ is the most appropriate due to the following considerations. The threshold for the onset of the instability is about $\dot{m}_0 = 0.26$ for $f = 0.9$, and scales as:

$$\dot{m}_0 = 0.02 [1 - f]^{-9/8} \quad (13)$$

(see Svensson & Zdziarski 1994 and note that their definition of \dot{m} differs from ours by a factor that accounts for the standard disk radiative efficiency, i.e., 0.06). It seems clear observationally that \dot{m}_0 should be larger by a factor of at least 5 than the value of $\dot{m} = 0.02$ corresponding to the transition from the gas- to radiation pressure-dominated regime in the standard theory. Indeed, if we assume that the maximum luminosity of $\sim 2 \times 10^{39}$ erg sec $^{-1}$ observed in GRS 1915+105 corresponds to the Eddington luminosity for this source, then the instability seems to exist only for $\dot{m} \gtrsim 0.1 - 0.2$. In addition, Galactic Black Hole Candidates (GBHCs) with a lower persistent luminosity, or weaker transient behavior, have not shown such violent instabilities as GRS 1915+105 does, and yet many of them are as bright as $0.1L_{\text{Edd}}$ (see, e.g., Barret, McClintock & Grindlay 1996). We will discuss the parameter f further in §4.3.1.

In Figure (5) we show the evolution of the integrated disk luminosity as a function of time for the nominal values of the parameters listed above and for $\dot{m} = 0.275$, 0.31, 0.5, and 1.5. In agreement with Equation (13), we find that for values of \dot{m} below 0.26 the disk is stable, because there is no radiation-pressure dominated zone in

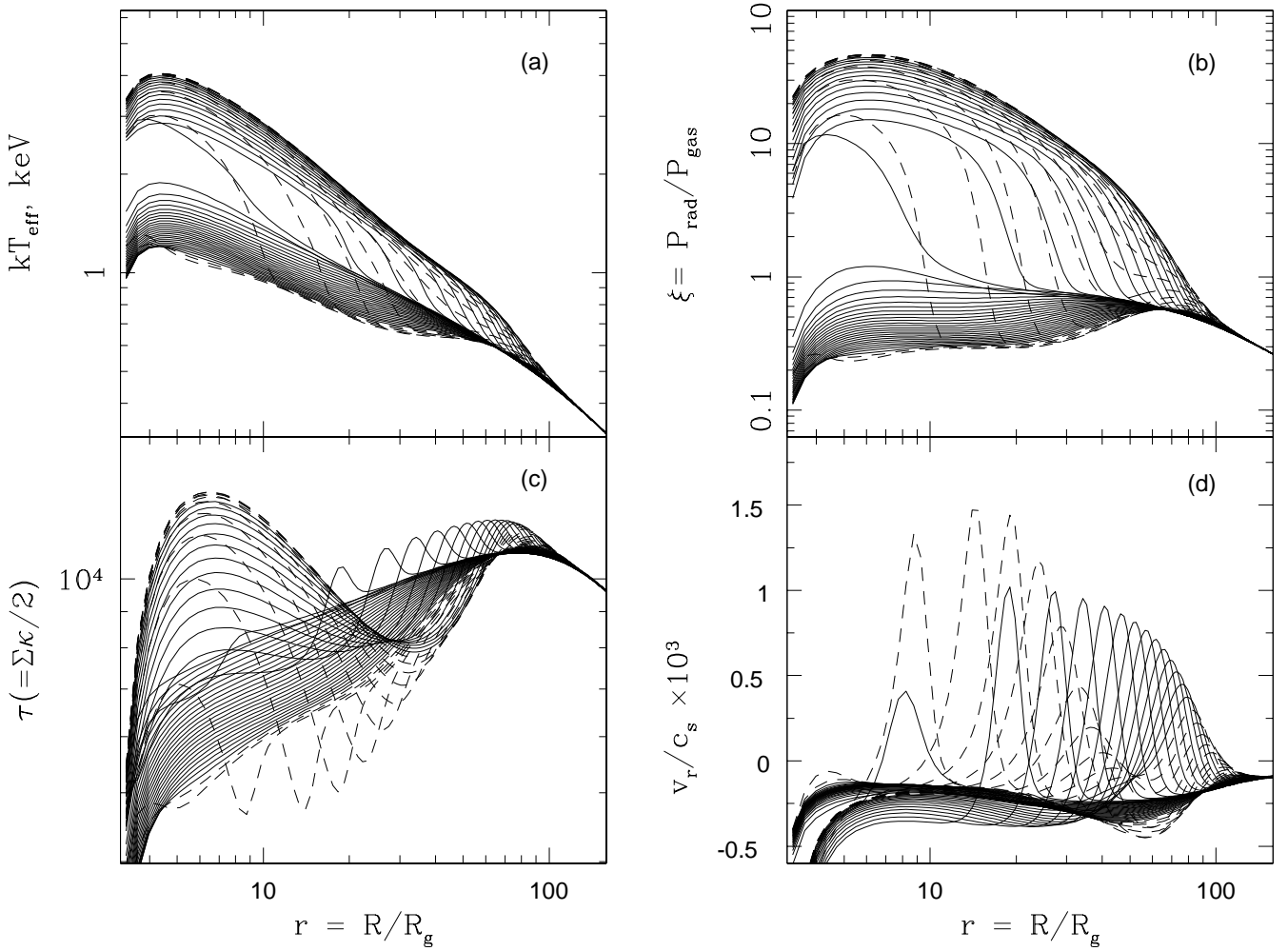


FIG. 4.— The evolution of (a) the disk temperature, (b) the ratio of radiation to gas pressure, ξ , (c) the Thomson optical depth, and (d) the ratio of radial flow velocity to the sound speed throughout one cycle for $f = 0$, $\dot{m} = 0.05$. Each curve is a snapshot of the parameter versus radius R , taken after each ~ 7.5 sec from about 670 to 1030 seconds in Fig. (3). The solid curves correspond to times when the luminosity increases with time (e.g., during the low state and during the rise to the maximum), whereas the dashed curves correspond to times when the luminosity decreases.

the disk. We also find, in general, that as the value of \dot{m} increases, the duty cycle (i.e., the fraction of time that the source spends in the high state) increases, from about 5% at $\dot{m} = 0.26$, to approximately 50% when $\dot{m} = 1.5$. Similarly, the ratio of maximum to minimum luminosity through the cycle grows with increasing \dot{m} .

The time for the disk to complete one of its cycles (defined as the cycle time) also increases with \dot{m} , except for very near the minimum value of $\dot{m} = 0.26$ where the instability first sets in; here the cycle time actually decreases with increasing \dot{m} . The reason is that there seems to exist a “critical excess mass” in the inner disk region, such that the instability will appear only when the mass in the disk exceeds this value. The rate for building up the excess mass is $\dot{m} - \dot{m}_0$, where \dot{m}_0 is the maximum stable accretion rate given by Equation (13), and therefore a small increase in \dot{m} above \dot{m}_0 can bring about a substantial decrease in the cycle time. For larger accretion rates, the cycle time starts to increase with increasing accretion rate, because a larger region of the disk is unstable, and it takes longer to clear the excess mass during the outburst.

4.3. Comparison to Observations of GRS 1915+105

We will now compare our results shown in Figure (5) with observations of GRS 1915+105. We should acknowledge at the start that it seems a daunting task to try to explain with a single model the diverse, unstable behavior exhibited by this source, but we expect to benefit from a comparison of even the gross properties of our model with the observations.

4.3.1. Gross Features

Panel (a) of Figure (5) is similar to Figure (1a) in that in both figures there exists a long phase of mass accumulation (the low state). Furthermore, an examination of the GRS 1915+105 data reveals that the cyclic limiting behavior disappears when the average count rate is lower than $\sim 5 \times 10^3$ counts/sec, so that there indeed exists a threshold accretion rate below which the instability does not operate. In simulations, the spiky nature of the outburst is explained by the fact that only a very narrow region in R within the disk is unstable, and it takes very little time to get rid of the excess mass in that region. The differences with Fig. (1a) are mainly due to the fact that

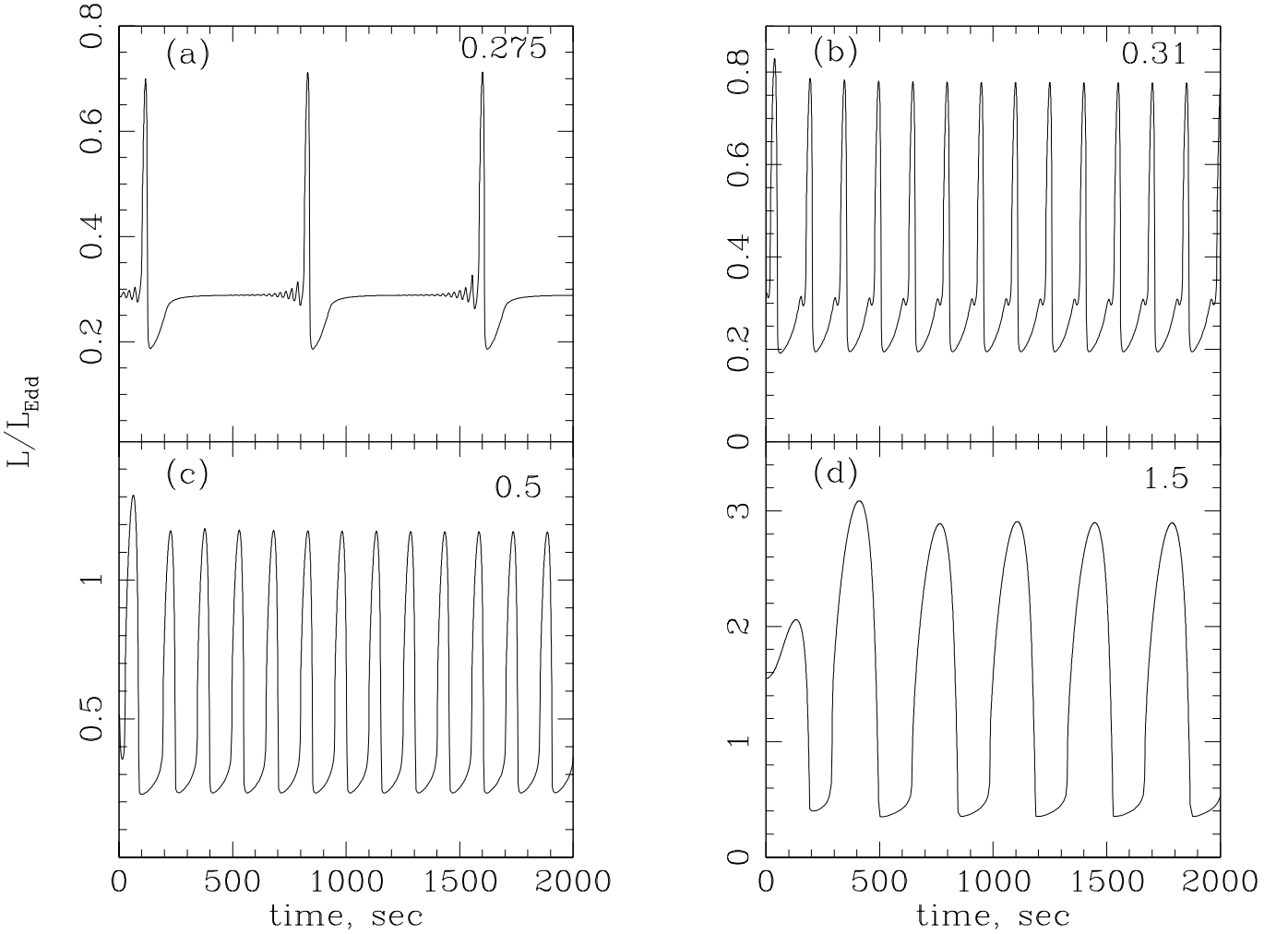


FIG. 5.— The light curves for an unstable accretion disk with a viscosity prescription given by Equation (12). The coronal dissipation fraction f is set to 0.9, $\alpha_0 = 0.01$, and $\xi_0 = 8$ for all tests. The dimensionless accretion rate \dot{m} is shown in the right upper corner of each figure.

an outburst in the data does not seem to completely clear the excess mass, and that more oscillations follow with a gradually declining amplitude, whereas in the simulations the hot state persists until all the excess mass is swallowed by the black hole.

Panel (b) of Fig. (1) is also somewhat similar to panels (b) and (c) of the simulations (Fig. 5). The progression of time scales and the average luminosity (i.e., roughly speaking, the count rate) from pattern (a) to (b) in Fig. (1) is similar to that from panel (a) to (b) in Fig. (5) as well. The physical reason for the cycle time getting shorter with increasing \dot{m} is that the excess mass can build up faster for larger accretion rates.

Next, panel (c) in Figure (1) is most interesting from the point of view that the high state is long lasting and is clearly stable at least for the first half. Panel (d) of the simulations can account for some of the properties of this variability pattern. In particular, the duty cycle increased in both the simulations and the data as the accretion rate increased. The cycle time did not increase nearly enough in the simulations, however. It could be made longer by choosing a smaller α_0 , but then the time scales in all the other panels would increase as well, which does not appear acceptable.

Also, a general trend seen in the first three panels (a-c) in both the data and the simulations is that the minimum of each light curve shows a slow gradual rise in luminosity before the instability sets in. This is a clear indication of the disk accumulating mass until it reaches a global instability.

We note that panel (d) of Figure (1) seems to be rather different from the other three variability examples. If the high state is again defined as the one with larger count rates, then a peculiarity of panel (d) is that the count rate first decreases and then increases by the end of a high state episode. This is the opposite of what is seen for the other states, such as that shown in panel (c) of Fig. (1). From a theoretical point of view, this is a highly significant observation. In all of our simulations, we observed that as the outburst progresses, the amount of mass in the inner disk region builds up because of the greater and greater inflow of mass from larger radii. Once in a given (high or low) stable state, the local disk luminosity is proportional to the local column density Σ , which can be seen from Figure (2). Therefore, in an outburst, the luminosity decreases only after the outer disk cools down and the influx of mass stops, leading to a decrease in Σ in the inner disk. Thus, the outburst profile in the simulations is such that

the second time derivative d^2L/dt^2 is always negative, not positive as seen in panel (d) of Figure 1. We do not see a clear explanation for this disagreement in the context of the current model, but we will show that there might be a natural cause for this phenomenon if a jet is allowed (§5).

Finally, we note that in a number of the panels in Figure (5), the first (and sometimes also the second) peak in the light curve is of slightly different intensity or duration than the peaks that come later in the sequence. This is simply a consequence of the disk adjusting to its quasi-steady cyclic pattern after starting from the imposed initial conditions that are given by the Shakura-Sunyaev solution corresponding to the mean value of \dot{m} .

Let us now discuss the rather extreme value for f invoked here, which requires that as much as 90% of the accretion power is carried out of the disk by processes other than the usual radiative diffusion. If this process is magnetic buoyancy or some other MHD process heating the corona, then there appears to be a contradiction with the observations of GRS 1915+105. The blackbody component in the spectrum of this source is generally small in the low state, but it can be dominant in the outburst state (Muno, Morgan & Remillard 1999). One could argue here that as much as 80 – 90% of the X-rays emitted by the corona towards the disk may be reprocessed into the soft disk radiation, (e.g., Magdziarz & Zdziarski 1995) if the reflection/reprocessing takes place in a *neutral medium* (neutral in the sense of high-Z elements like oxygen and iron, that are important for the reflection spectrum). Thus, in principle, the blackbody flux could exceed that in the non-thermal component by the ratio $\sim (2-f)/f$ (see Eqs. 1–5 in Haardt & Maraschi 1991 with their parameters $a \simeq 0$ and $\eta \simeq 1/2$). The rather high inferred disk temperature in GRS 1915+105, e.g., $kT \sim 2$ keV (Belloni et al. 1997a), rules out the possibility of neutral reflection, however. As found by Nayakshin & Dove (1998) and Nayakshin (1998), the integrated albedo of the reflected spectrum in the case of a strongly ionized disk can be much higher than the standard 0.1-0.2 of the neutral reflector (i.e., $a \gtrsim 0.5$ in Eqs. 1–5 of Haardt & Maraschi 1991), and thus it seems difficult to have f as large as 0.9 given the large amount of soft power observed from the disk.

A possible way out of this dilemma is that the high value of f does not necessarily represent the energy flux from the disk into the corona. Indeed, Equation (9) states that the energy transport out of the disk may be $(1-f)^{-1}$ times faster than that given by the standard diffusion of radiation. Convection of energy in the vertical direction (e.g., Bisnovatiy-Kogan & Blinnikov 1977; Goldman & Wandel 1995; and references therein) is one physical mechanism that can speed up the transfer of energy out of the disk. MHD waves dissipating their energy before they reach the corona could be another. In addition, there is no proof that the vertical averaging procedure (i.e., a one zone approximation) used in the standard accretion disk theory does not lead to a substantial underestimation of the vertical radiation flux out of the disk. For example, if $F_{\text{rad}} = (cP_{\text{rad}}/\tau_d)\zeta$, where $\zeta \sim \text{few}$, then \dot{m}_0 becomes $\dot{m}_0 = 0.02\zeta^{9/8}$ (see SZ94), and thus one may have \dot{m}_0 as large as that observed in GRS 1915+105 due to a faster or an additional disk cooling mechanism rather than due to a transfer of most of the disk power into the corona.

4.3.2. Rapid Flickering

It is notable that panel (c) of Fig. (1) shows rapid chaotic oscillations as fast as \sim tens of seconds at the end of the high state, whereas our simulations do not show a similar behavior. Furthermore, note that the rise/fall time scales are shorter in the data than they are in our model. It appears that the heating of the unstable region in GRS1915 happens on a time scale that is very much shorter than the cycle time. By contrast, the outermost part of the unstable region of the simulated disk becomes unstable only after $\sim 1/2$ the duration of the hot phase, that is of the order of the disk viscous time for the high luminosity cases.

One explanation here could be that these fast oscillations are failed attempts by the disk to make a state transition from the high to the low state. Further, during these fast oscillations the disk is always brighter than it is in the low state, which could be interpreted as an indication that only a part of the disk (most likely the innermost region) in GRS 1915+105 takes part in these rapid oscillations, whereas the rest of the unstable region is still on the upper stable branch of the S-curve. For this to be true, the inner disk must be able to decouple to some extent from the rest of the unstable disk, and be variable on a much shorter time scale than the outer disk.

To test this idea, we have carried out several simulations in which the α -parameter is a decreasing function of radius. Our hope is that in this case, since α in the inner disk is larger than that in the outer disk, the time scale for oscillations in the inner disk may be much shorter than the overall viscous time, which has the dependence $t_v \propto \alpha^{-1}$ (e.g., Frank et al. 1992). In Figure (6) we show one such simulation, in which the viscosity parameter was chosen to be $\alpha(\xi, r) = \alpha(\xi)[0.1 + \{1 + (r/8)^3\}^{-1}]$. This functional form allows the α -parameter to be roughly $\alpha(\xi)$ in the inner disk region ($R \leq 8R_g$), and to be $\sim 0.1\alpha(\xi)$ for $R > 8R_g$. The presence of these two time scales is obvious just from a perusal of the resulting light curves. Oscillations of the inner disk produce the precursor seen before each major outburst in Fig. (6). Its relative magnitude is small because the amount of excess mass stored in the inner disk is small compared to that in the outer disk. Furthermore, in the simulations the inner disk decouples from the outer one only at the beginning of the outburst, not at the end as is seen in the GRS 1915+105 data. This is due to the fact that once the outer disk makes a transition to the high state, the large mass supply to the inner disk forces the latter to go into the high state as well and remain there. In summary, varying the α -parameter with radial distance does not appear to be a viable explanation for the rapid chaotic oscillations seen in the data which are superposed on the more regular long time scale disk evolution.

An alternative way of explaining the fast oscillations could have been provided if the heating/cooling fronts stall and are reflected back as cooling/heating fronts. This behavior was observed in simulations of the classical thermal ionization disk instability by Cannizzo (1993, see text above his Equation 5), where it happened to be an unwanted result. However, we have not been able to see such stalled transition fronts (except for the case presented in Fig. 6), which should not be too surprising, due to the

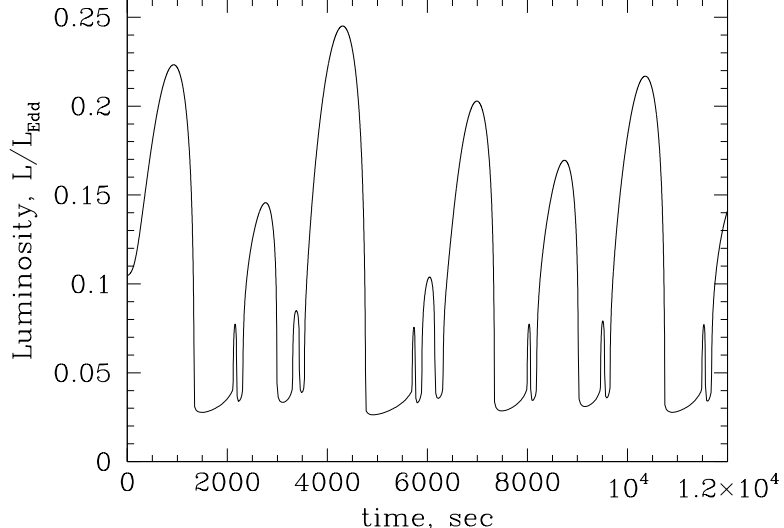


FIG. 6.— The effects of varying the α -parameter with radius, according to $\alpha(\xi, r) = \alpha(\xi)\{0.1 + [1 + (r/8)^3]^{-1}\}$. This effectively gives two different viscous time scales, which is clearly seen in the resulting light curves. See text for discussion.

fact that the underlying physics of the ionization instability and the one explored in this paper are vastly different, and one does not expect a direct correspondence between these two instabilities.

Although we will not present any light curves, we should mention that we have also attempted to allow the fraction f to be a function of ξ , since the transition from $\xi < 1$ to $\xi > 1$ means a substantial change in the physical conditions in the disk. Our hope was that the freedom in choosing $f(\xi)$ might help to reproduce the disk flickering. However, all our attempts in this regard (with f decreasing or increasing across the transition in ξ) have been unsuccesful.

5. PLASMA EJECTION FROM THE INNER DISK

Although our model is able to reproduce a number of the general trends seen in the light curve of GRS 1915+105, the rise/fall time scales are always shorter in the data than they are in the simulations. The fast rises and falls are perhaps the reason why the profile of an outburst in some of the actual light curves of GRS 1915+105 (e.g., panel (c) of Fig. 1) is reminiscent of a square-wave like shape rather than the rounded shapes that an outburst has in the simulations (see Fig. 5d). The difference between our simulations and the data appears important enough to us to require the addition of a new feature to our model and test whether it can bring the theory closer to the observations.

The following considerations have guided us in choosing the additional ingredient in our model. The speed with which the hot state propagates outward in the accretion disk is equal to the speed of the transition wave, which was studied analytically by, e.g., Meyer (1984) and numerically by Menou, Hameury & Stehle (1998). Both of these studies find that the propagation speed of the transition wave is $v_t \simeq \alpha c_s$. The time scale for the transition front to traverse an unstable region of size R is $t_t \sim R/\alpha c_s = (R/H)t_{th}$, i.e., the transitions in the disk actually take R/H times longer than the thermal time scale of the outermost part of the unstable disk region. This is the reason why the

rises and falls take too long in the simulations compared to the data.

However, notice that during the initial stage of the transition from the low to the high state, the luminosity rises quite rapidly in the simulations (see Fig 5d), at a rate probably as fast as that seen in the data. Now, if some physical process were to “cut” the simulated light curves at, say, $L = L_{\text{Edd}}$, so that anything emitted by the disk above this value is *not seen* by the observer, then the outburst profile would be much more consistent with the data.

To find a process able to “cut” the light curve, we should recall that powerful plasma ejections are known to occur in GRS 1915+105 (e.g., Mirabel and Rodriguez 1994). Recently, Eikenberry et al. (1998), Mirabel et al. (1997) and Fender & Pooley (1998) have shown that there exists a strong link between the X-ray emission and emission in the infrared and radio frequencies. The radio and infrared emission is attributed to plasma ejection events taking place in the innermost part of the disk. The minimum power deposited at the base of the jet (that may consist of individual ejection events) was found (e.g., Gliozzi, Bodo & Ghisellini 1999) to be as high as $L_j \sim \text{few} \times 10^{40}$ erg sec $^{-1}$ for the event first discovered by Mirabel and Rodriguez (1994). During other observations (e.g., Eikenberry et al. 1998), the radio fluxes were a factor of ~ 10 lower than the ones observed by Mirabel & Rodriguez (1994), which still may require $\sim \text{few} \times 10^{39}$ erg sec $^{-1}$ ejected into the jet, which is as large as the largest X-ray luminosities produced by the source. Thus, if one were to model these plasma ejections in the framework of our model, one would have to allow for a significant portion of the accretion *energy* to be diverted into the jet.

From here on, we will therefore assume that the total accretion disk power L_t consists of two parts: the first is the X-ray luminosity L_x , that is equal to the sum of the thermal disk and non-thermal coronal luminosities; and the second part L_j is the “jet power”, i.e., the energy ejected into the jet. For simplicity we further assume that the jet power is not seen in X-rays, and appears only in the radio or other non-X-ray wavebands. As before, the locally produced total disk power is given by Equation (9), where

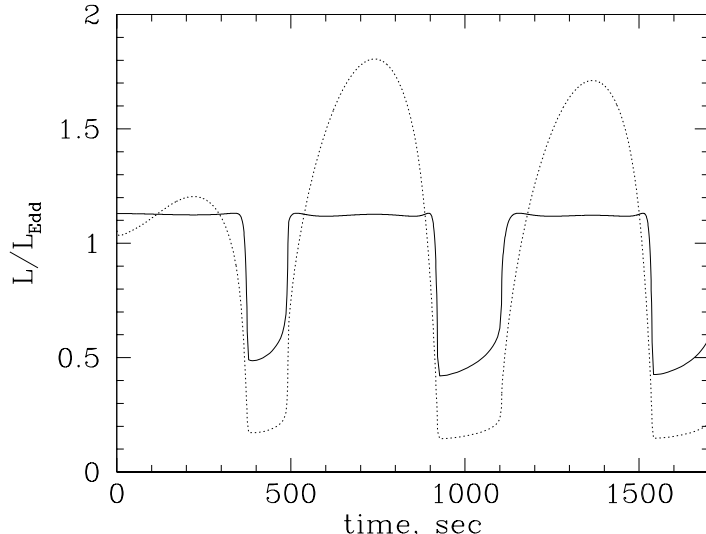


FIG. 7.— The light curve for the disk, corona and jet model. The solid curve shows the X-ray luminosity, whereas the dashed curve shows the overall disk power (i.e., X-ray luminosity plus the energy ejected in the jet) scaled down by a factor of 3 for clarity of presentation. The accretion rate used for this test is $\dot{m} = 3$, and the fraction of the power emerging as X-rays depends on the overall disk power $\Lambda \equiv L_t/L_{\text{Edd}}$ as $\eta_x = [1 + (\Lambda/2)^2]^{-1}$. The viscosity prescription and other parameters of the model are the same as those used in Fig. (5).

we will again suppose that $f = 0.9$. The jet luminosity is then

$$L_j = 2 \times 2\pi R_g^2 \int_3^{r_{\text{max}}} r dr f \eta_j F^- \quad (14)$$

where $0 \leq \eta_j \leq 1$ is the fraction of power that escapes from the disk into the jet. This parameter (η_j) may be a constant, or it may be a function of local disk conditions or a function of some global variable, e.g., the total disk power L_t . Since the importance of advection relative to the radiative cooling is roughly given by the ratio $(H/R)^2$, and since according to our discussion in Appendix A $H/R \ll 1$ in this source, the advection of energy is not important in our model. Thus, the observed X-ray power L_x will consist from the disk power (fraction $1 - f$ of the total disk power) and the coronal luminosity which is given by an equation analogous to Equation (14) except with a parameter $\eta_x = 1 - \eta_j$ instead of η_j inside the integral. To eliminate any ambiguities of our approach, we note that the accretion power is divided among the disk, the corona, and the jet as $1 - f$, $f\eta_x$ and $f\eta_j$, respectively.

We should also mention that the amount of mass carried away by the jet is small compared to that accreted into the black hole, so we neglect the former in the mass conservation (eq. 4). The point here is rather simple: if the ultimate source of the jet power is the underlying accretion disk, then to produce one relativistic proton in the jet, many protons in the disk must transfer their gravitational energy (which is small compared with their rest mass) to that one jet proton. These protons will therefore have to sink into the black hole in order to send one proton into the jet. More precisely, the mass outflow rate is $\dot{M}_j \lesssim L_j/\gamma_j c^2$, where $\gamma_j \sim \text{few}$ is the terminal bulk Lorenz factor of the jet. This is to be compared with the accretion rate through the disk, that is equal to $\dot{M}_d = L_t/\epsilon c^2$, where ϵ is the “radiative” efficiency of the disk and L_t is the total disk power. Accordingly,

$$\frac{\dot{M}_j}{\dot{M}_d} \lesssim \epsilon \gamma_j^{-1} \frac{L_j}{L_t} \lesssim 0.1, \quad (15)$$

since $\epsilon \lesssim 1/6$. This estimate is quite conservative. For example, if the jet power is dominated by magnetic fields or by electron-positron pairs, then the mass carried away in the jet is even smaller. A similar consideration allows us to neglect the angular momentum outflow from the disk into the jet. We point out however that the latter approximation depends on the model of the jet; if the jet particles actually gain a considerable amount of the angular momentum as they are streaming away from the disk, then the torque exerted by the jet on the disk may become non-negligible. We plan to explore these effects in future work.

Eikenberry et al. (1998) found that the ejection events were absent in the low state and started at the onset and during the high state. We thus will accept a parameterization of η_j such that it is close to zero when the disk is in the low state, and it is relatively large (but still smaller than unity, of course) when the disk is in the high state. We now explore three different illustrative prescriptions for the function η_j to show the possible effects of the disk power being diverted into a jet.

5.1. Test 1

Let us assume that the fraction η_j is described by the following (somewhat arbitrarily chosen) function:

$$\eta_j = 1 - \frac{1}{1 + (\Lambda/2)^2}, \quad (16)$$

where $\Lambda \equiv L_t/L_{\text{Edd}}$ is the total power of the source in terms of its Eddington luminosity. This equation is qualitatively reasonable since one expects particles to be ejected from the disk when the luminosity L approaches (and then exceeds) the Eddington limit. While the radiation may not be the ultimate driving power of the jet, the radiation pressure can cause more matter to be ejected and possibly produce stronger jets. We show in Figure (7) the resulting X-ray light curve (solid line) and the total disk luminosity L_t (represented by a dashed curve; scaled down by the

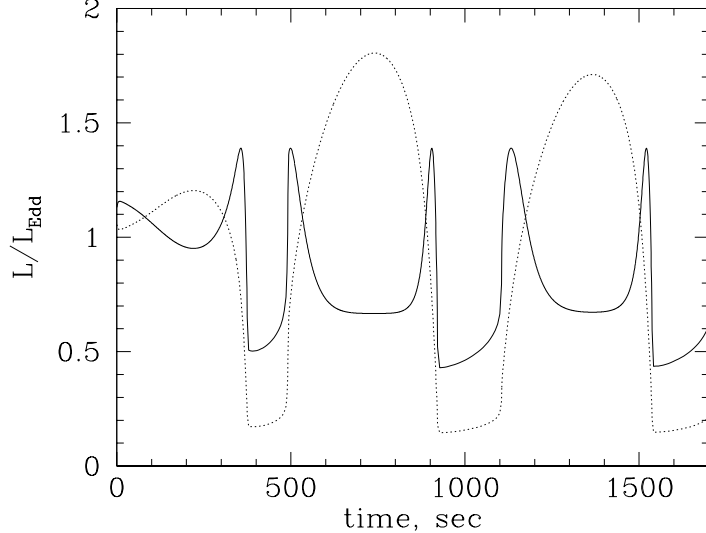


FIG. 8.— Same as Fig. (7), except the fraction of power going into X-rays is now given by $\eta_x = [1 + (\Lambda/3)^2 + (\Lambda/3)^6]^{-1}$. Notice that during the high state, the X-ray light curves exhibit local minima rather than maxima.

factor of 3 to fit the figure) for an accretion rate $\dot{m} = 3$. Note that the overall luminosity curve is the same as we would have obtained with our basic model for the same choice of f and \dot{m} , but with no jet ejections (see §§3 & 4).

The shape of the outburst indeed becomes more like a square-wave, and thus the rises and falls appear to be sharper than they were for the model with $\eta_j = 0$, thus making it possible to reproduce this feature of the observed light-curves (in particular, panel (c) of Fig. 1).

5.2. Test 2

As a second example, we test the following prescription for the jet power:

$$\eta_j = 1 - \frac{1}{1 + (\Lambda/3)^2 + (\Lambda/3)^6}. \quad (17)$$

(This prescription, in contrast to the one given by eq. [16], was chosen among several that we tested to reproduce the panels (c) and (d) of Fig. [1] simultaneously as described in §5.3). The corresponding X-ray light curve and the total luminosity of the system are shown in Figure (8). One notices that the profile of the outburst in X-rays is now inverted with respect to the actual disk power. When the disk produces most of the energy output, the X-ray light curve actually has a local minimum, since most of the energy is ejected into the jet during that time. This effect may be responsible for the “strange” shape of the outburst seen in panel (d) of Fig (1).

5.3. Test 3

As a final example we present a sequence of light curves produced by our model with a fixed prescription for the jet energy fraction η_j and with the accretion rate being the only parameter that is varied. The functional dependence of η_j is again given by eq. (17). Further, motivated by the fact that the X-ray emission can fluctuate wildly when it is in the high state (see Fig. 1), whereas it does not fluctuate as much in the low luminosity state, we allow the fraction f carried away from the disk other than by the usual radiation diffusion to fluctuate around some mean.

Numerically, the f -factor will now contain a *random* variable part $f_1 = 0.03$, such that $f_1 \ll f_0$:

$$f = f_0 + f_1 \mu g(r) \frac{\Lambda^2}{4 + \Lambda^2}, \quad (18)$$

where f_0 is the constant part fixed at the previously selected value of 0.9, μ is a random number distributed uniformly between -1 and +1 (a new value of μ is randomly chosen every 3 seconds), and $g(r) \equiv r_1^4/(r^4 + r_1^4)$ is a function of radius r such that it is unity in the inner disk and it approaches zero for $r > r_1 = 30$. The latter radial dependence is introduced simply to avoid complications with the outer boundary condition at $r = 10^3$, where we set the disk structure to be that given by the gas-dominated Shakura-Sunyaev configuration with a constant $f = f_0$ (see §3.1). The shape of the function $g(r)$ is almost completely irrelevant for the resulting light curves as long as r_1 is large, since most of the disk power is liberated in the inner disk region. Finally, although the second term on the right hand side of the Equation (18) appears to be complicated and model-dependent, its presence is not required and serves only to make the light curves look somewhat more random. None of the final conclusions of this paper depend on the particular choice for the random part in f .

Figure (9) shows the resulting X-ray light curves for four different accretion rates. It is worthwhile comparing Figure (9) with Figure (5), in which the plasma ejections and random fluctuations in f were absent. The case with the accretion rate just above \dot{m}_0 (i.e., panel c in Fig. 5) has not been affected as strongly as that with the higher accretion rate; this is of course due to the fact that little energy is ejected in the jet in the former case compared with the latter. Yet panels (a) and (c) do look more chaotic, which is entirely due to the fluctuating part in the fraction f (see Eq. (18)).

Analyzing panels (b) and (d) of this figure, one notices that it turns out to be possible to reproduce both the sharp square-wave like pattern (c) and the “inverted” pattern (d) of Figure 1 with the *same* prescription for η_j . It is the same process, i.e., the plasma ejection, that allows

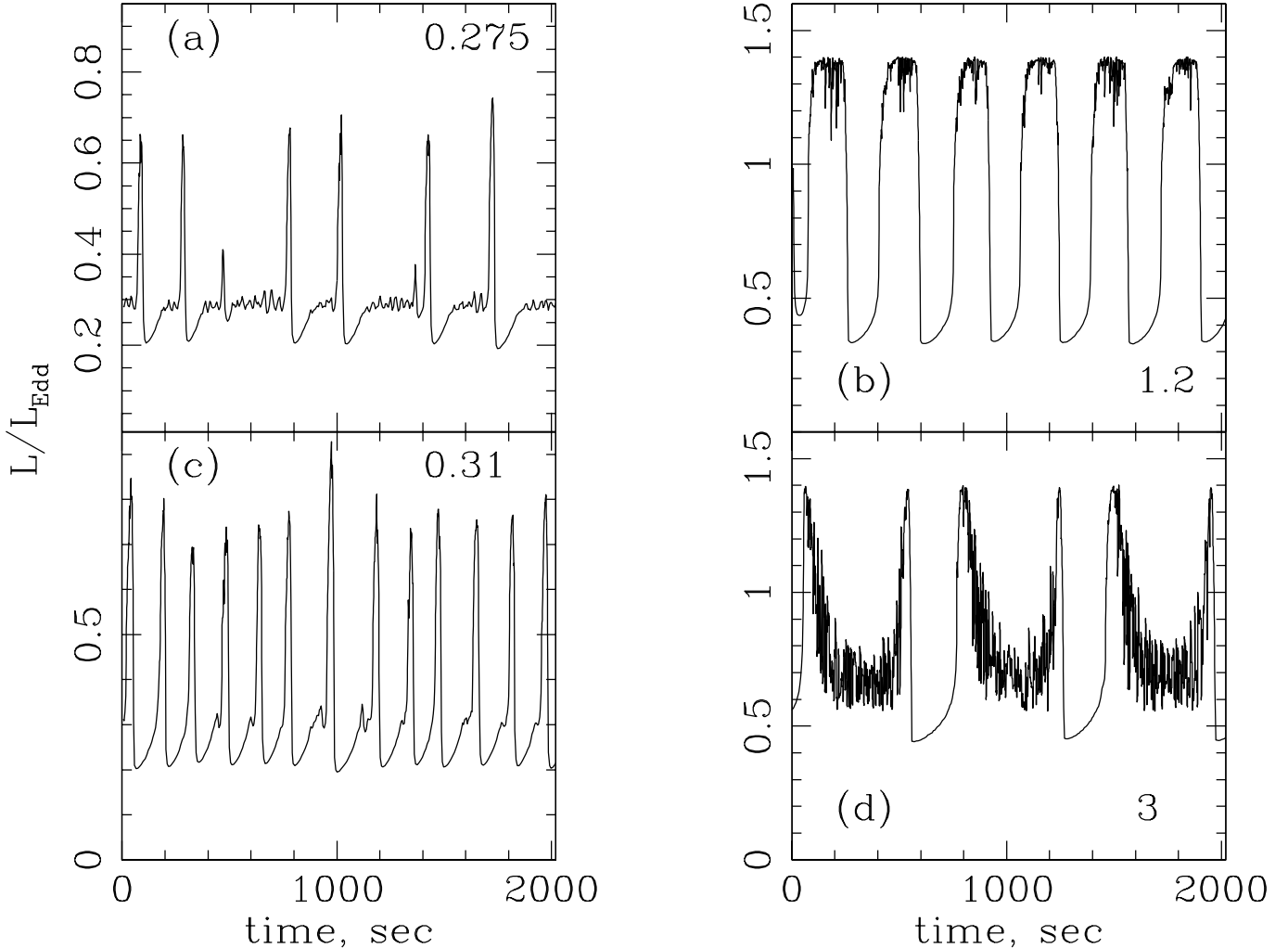


FIG. 9.— The light curves for the unstable accretion disk with a viscosity prescription given by Equation (12), and with the fluctuating corona and plasma ejections. The fraction f is given by Equation (18), $\alpha_0 = 0.008$, and $\xi_0 = 8$ for all the tests. The dimensionless accretion rate \dot{m} is shown in the upper right or lower right corner of each panel.

our model to better reproduce the data (panels [c] and [d] of Fig. 1); the only difference being that in panel (d) the ejected fraction of the disk energy is much greater than in panel (b). For the completeness of presentation, we also plot the jet power L_j with a dotted curve in Fig. (10) corresponding to the simulation presented in panel (b) of Fig. (9).

Given the relatively good agreement between the model and the observations of GRS 1915+105, we believe that we now have a better handle on the key characteristics of accretion in this source. While we feel less confident about the origin of the S-curve in the $\Sigma - T_{\text{eff}}$ space, we think that the geometry of the accretion flow in GRS 1915+105 is that of a geometrically thin and optically thick flow (see §A). Most of the X-ray luminosity is produced in an optically thin corona, that can cover the entire inner disk or consist of localized transient magnetic flares (e.g., Haardt, Maraschi & Ghisellini 1994; Nayakshin & Melia 1997; Nayakshin 1998). In the latter case, the fraction f of the power transported from the disk into the corona and the jet must be thought of as a time averaged variable. Further, we believe that plasma ejection events must be an integral part of the accretion process, and are likely to

be the result of an excessively large radiation pressure. We will discuss this issue in a broader context in §7.

6. COMPARISON TO PREVIOUS WORK

Belloni et al. (1997a,b) were the first to fit the spectrum in GRS 1915+105 with a two-component model, consisting of a multi-temperature disk-blackbody with a variable inner disk radius plus a power-law. Very importantly, these authors found that most of the complex spectral variability can be explained by a rapid change in the disk inner radius R_{in} and a corresponding change in the temperature of the disk at R_{in} . They have also shown a correlation between the disk filling time scale and the inferred radius of the inner disk.

Our results are qualitatively similar to the framework of the disk instability discussed by Belloni et al. for GRS 1915+105 since in the low state the inner disk is quite dim (up to a factor of 10-30, see Figure 11) compared with what it should have been if the disk were stable. Thus, the inner part of the disk can be largely unobservable and can be said to be “missing”. At the same time, in the high state, the inner disk is brighter than its equilibrium luminosity by typically a factor of a few, which

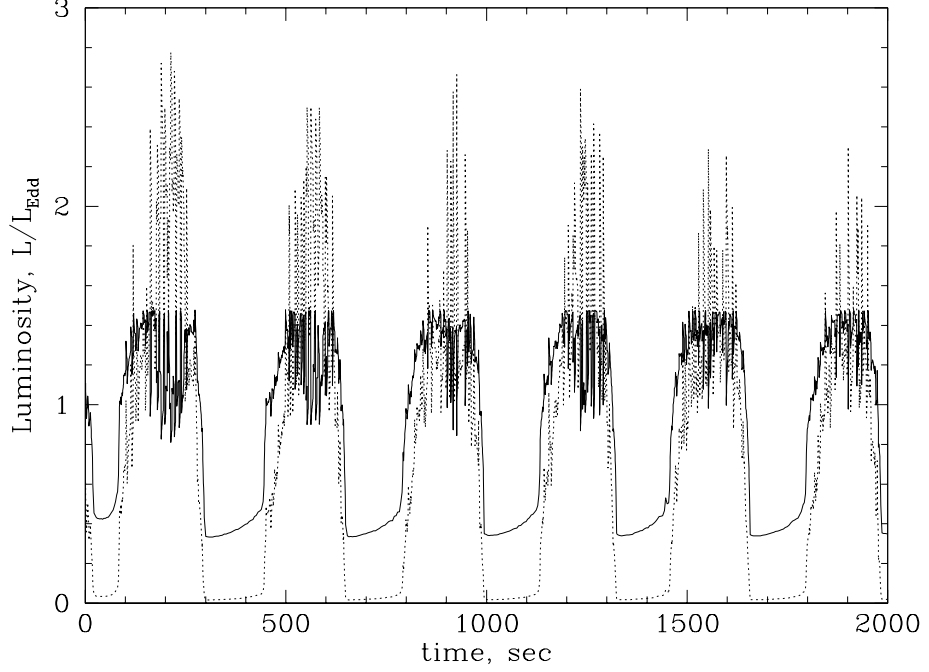


FIG. 10.— The X-ray luminosity (solid) and plasma ejection power (dotted) corresponding to the $\dot{m} = 1.2$ panel of Figure (9).

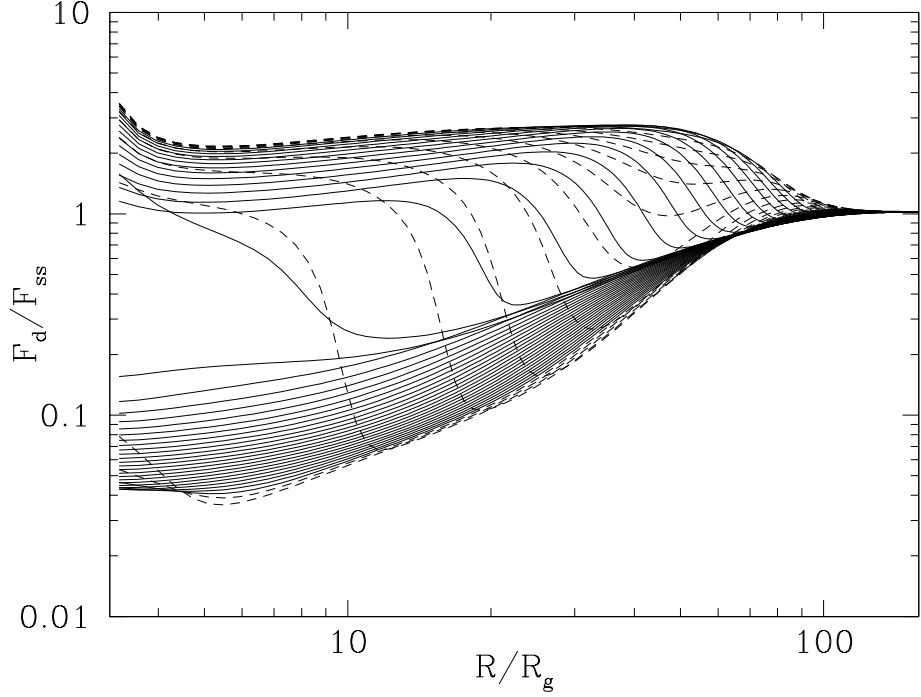


FIG. 11.— The ratio of the local X-ray luminosity to the luminosity of a standard Shakura-Sunyaev disk with the given accretion rate through one complete cycle. The model and its parameters are those used to generate Figure 4 (the disk behavior in the tests presented in Fig. 9 is similar to the one shown here, except for appropriate changes in the extent of the unstable region in the disk). Note that the inner part of the disk can indeed be very dim compared to its standard value and thus appear to vanish below observability.

may make the outer part of the disk (that is stable and so has just the “normal” flux) seem comparatively dim. Under these conditions, it may be non-trivial to distinguish observationally between a disk where the temperature is a continuous function of R ($T \propto R^{-3/4}$) and a disk where the temperature is lower than expected in the outer part of the disk, since the outer disk carries a small fraction of the overall luminosity. In addition, the inner disk is never

completely empty of mass in our model, although the difference between the inner disk surface density in the high versus that in the low state can be a factor of \sim few to 10 (see Fig. 4c).

Note that R_{in} as defined by Belloni et al. should be identified with the largest radius reached by the heating wave in our simulations. More specifically, during the high state, R_{in} should be defined as the radius of innermost sta-

ble orbit, whereas during the low state it is approximately equal to the largest radius in the disk in which $P_{\text{rad}} = P_{\text{gas}}$ (i.e., $R_{\text{in}} \simeq 100$ for Fig. 11). Our values of R_{in} are in general much larger than those obtained by Belloni et al. The value of R_{in} inferred from the observations could be larger if one were to fit the GRS 1915+105 emission with a more complicated (and likely more realistic) spectrum than a multi-temperature blackbody appropriate for a Shakura-Sunyaev disk. Moreover, for the high accretion rates observed in this source, the disk may become effectively optically thin and thus radiate as a modified (rather than a pure) blackbody (see discussion in Taam et al. 1997). Since blackbody emission produces the maximum flux for a given temperature, the modified emission would require a larger R_{in} . Finally, the values of R_{in} obtained by us would presumably be smaller for a Kerr black hole. We plan to address this question in the future.

Belloni et al. (1997b) showed that the outburst duration is proportional to the duration of the preceding quiescent state, but there is no correlation between the former and the quiescent time after the burst. Profiles of outbursts in our model are rather regular, so we believe we see a correlation among these three quantities in contrast to the Belloni et al. results. On the other hand, in many observations (other than the one presented in Belloni et al. 1997b) GRS 1915+105 does not show a good correlation between the duration of the outburst and the preceding quiescent phase (T. Belloni 1999, private communication).

7. DISCUSSION

We have systematically analyzed the physical principles underlying the behavior of GRS 1915+105, and have arrived at several important conclusions regarding the nature of the time-dependent accretion flow in this system. As discussed in Appendix §A, geometrically thick advection-dominated flows are unacceptable for this source, since they would produce burst-like instabilities with a very small duty cycle compared to those seen in the data, for accretion rates smaller than the Eddington value. To produce outbursts as long as ~ 1000 seconds, geometrically thick accretion flows must have implausibly small values of α . However, if the accretion rate is highly super-Eddington, then a thick ADAF disk could yield outbursts with a reasonable duty cycle (~ 0.5). But since the viscous time scale for geometrically thick disks is as short as the thermal one, their light curves would be rather smooth which again contradicts the data (see, e.g., panels c & d of Fig. 1). It is also unclear how the observation (e.g., Belloni et al. 1997a,b; Muno, Morgan & Remillard 1999) that the disk extends down to the innermost stable orbit during the high state can be reconciled with the structure of a geometrically thick, hot and optically thin flow.

For these reasons, the standard cold accretion disk with a modified viscosity law, a corona, and plasma ejections seems to be the only reasonable choice. As we have shown in this paper, this geometry indeed allows one to obtain rather good general agreement between the theory and observations, and to understand particular features of the light curves in terms of fundamental physical processes.

Nevertheless, a critical reader may question whether the relatively large number of parameters introduced by us in this work allows us to pin-point actual values of these parameters. We believe that the answer to this question is

“yes”, because spectral constraints, used very sparingly here, may prove to be quite restrictive in future studies. For example, we have shown only the total luminosity light curves in this paper, whereas the data also contain a wealth of information about the spectral evolution in GRS 1915+105 (Belloni et al. 1997; Muno et al. 1999). If future observations also provide more examples of the disk-jet connection (e.g., Eikenberry et al. 1998), then we have a means of constraining the dependence of both η_j and the total fraction f on the disk luminosity. Further, one should also attempt to explore the fact that other transient and persistent black hole sources do not exhibit instabilities similar to GRS 1915+105, at least not to the same extreme degree. Thus, putting all these observational and theoretical constraints together may be quite effective in limiting the theoretical possibilities for the instability and the coronal and jet activity.

As an example of the need for a detailed study of the spectra and QPOs in the context of our model, we point out the following. From the results of Muno et al. (1999) it appears that QPOs are present when the power-law component dominates the spectrum, which usually happens in the low state (“low” means the lower count rate). Further, these authors find that for the burst profiles similar to the one shown in Fig. 1(d), the QPOs are present during the “high” state, which is opposite to most of the other cases. If QPOs indeed track the presence of a vigorous corona, this would imply that although our panel (d) in Fig. (9) looks similar to Fig. 1(d), it does not represent the actual situation very well. Namely, the data seem to imply that the higher count rate states actually have lower accretion rates through the inner disk than the lower luminosity states (because excess luminosity escapes into the jet). It is thus possible that plasma ejections occur during the sharp dips in Fig 1(d) rather than during the longer phases (e.g., from ~ 420 to ~ 960 sec in this figure). The “M-shape” of the outbursts in Fig. (1d) may then be understood because these would be the low states as tracked by the accretion rate, and the low states of the three other panels (a-c) of Fig. (1) show similar shapes albeit with lower count rates. Although we have not yet made a detailed study of this suggestion, we can probably accommodate it within our model, but only if we allow the parameters in our viscosity law to depend on the disk luminosity. *Note, however, that in either case we must require plasma ejections from the inner disk in order to understand panel (d) of Fig. (1).*

The discussion above of course bears on the particular choice of the viscosity law that we have made in this paper. We emphasize that our model is still rather empirical and we have not identified the actual physics of the viscosity law in GRS 1915+105. The real physics might well be yet more complex, and in fact, the existence of the S-curve might be due to other than radiation pressure instabilities, perhaps involving an effect that we do not currently understand. However, based on the results presented in this paper, we feel confident that there is an S-curve in this source, and that this curve can be modeled approximately by the viscosity law given by equation (12).

A clear shortcoming of our work is the use of a non-relativistic disk around a non-spinning black hole. We plan to improve this in our future work. We expect that this will change the “reasonable” values of the parameters

that we used, such as the fraction f , and the inner disk radius, of course, but that it will not affect the general nature of our conclusions.

The authors thank T. Belloni, R. Taam, M. Muno, E.

Morgan, R. Remillard, E. Vishniac and D. Kazanas for useful discussions. This work was supported in part by NASA Grants NAG5-8239 and NAG5-4057, under the Astrophysics Theory Program.

APPENDIX

A. ON THE GEOMETRY OF THE ACCRETION FLOW IN GRS 1915+105

In almost any accretion disk theory, the ratio of the disk half thickness H to the radius R becomes comparable to unity when the accretion rate approaches the Eddington limit, which is almost certainly the case for this source. However, the data strongly suggest that $H/R \ll 1$ in GRS 1915+105. Indeed, a state transition in the unstable portion of the disk cannot occur faster than one thermal time scale, since the gas needs to be heated up or cooled down substantially to go from one branch of the solution to the other. Let us now consider panel (c) or (d) of Figure 1, since these are the highest luminosity cases, where H/R should be the largest and so time variability constraints are the strongest there. By looking at these two panels, one notices that the observations require that the thermal time scale be smaller than about 10 seconds ($t_{\text{th}} \lesssim 10$ sec), whereas the cycle time is of the order of a thousand seconds. The cycle time should be associated with the disk viscous time scale, i.e., the time during which the disk surface density Σ can change appreciably (and so cause a state transition), which is $t_{\text{visc}} \sim (R/H)^2 t_{\text{th}}$ (see §5.8 of Frank et al. 1992). This implies $(H/R) \lesssim 0.1$

ADAFs are ruled out for GRS 1915+105

ADAF configurations (see, e.g., Narayan & Yi 1995) have $H/R \simeq 1$ even for very low accretion rates. For this reason, ADAFs are ruled out for GRS 1915+105. Since by definition the thermal time scale in ADAFs is longer than the viscous time scale, the rise and fall in the light curve produced by an ADAF always would be very gradual and of the same duration as the whole outburst phase. More specifically, an ADAF is like a slim disk, in the sense that it can produce short spiky bursts, because t_{visc} in the high state can be quite short (see Figures 7-9 in Szuszkiewicz & Miller 1998), but it cannot explain *long outburst cycles with very fast transitions*, such as the ones seen in panels (c,d) of Figure 1. Furthermore, the viscous time is exceedingly short for disks where advection is important: $t_{\text{visc}} \sim \alpha^{-1} t_{\text{dyn}} \sim 3 \times 10^{-3} M_1 \alpha^{-1}$ sec, where M_1 is the black hole mass in units of M_\odot . This numerical value of the viscous time scale corresponds to $r \equiv R/R_g = 10$ (since this appears to be the appropriate value based on observations by, e.g., Belloni et al. 1997a,b and Muno et al. 1999). Thus, to reconcile this with the observed viscous time scale of $\sim 10^3$ sec, one should expect a very small α -parameter, i.e., $\alpha \sim 3 \times 10^{-6}$, which seems rather unrealistic. Moreover, even if one *can* neglect all the interactions between electrons and protons except for Coulomb collisions (otherwise ADAFs would never form), as well as omit the Ohmic heating of electrons (see Bisnovatyi-Kogan & Lovelace 1998; Quataert 1998), one still has the constraint that ADAFs can exist only below $m \lesssim \alpha^2$ (see Narayan & Yi 1995), which is clearly too small for GRS1915 if $\alpha \sim 3 \times 10^{-6}$.

Hot central region

An alternative model that has been suggested for generating X-rays in a black hole accretion disk invokes the presence of a central quasi-spherical emission region that is optically thin and hot. The main appeal of this type of model is its geometrical simplicity, which however ends immediately when one attempts to supplement this picture with realistic physics. We are unaware of any detailed and successful attempt to model this central source (i.e., with the inclusion of energy and pressure balance for the hot plasma), except for ADAFs and the two-temperature model for Cyg X-1 (Shapiro, Lightman & Eardley 1976). The first model is unacceptable for the reasons discussed in §A.1, whereas the second model is known to be thermally unstable (and does not contain the two upper and lower stable solutions needed for GRS 1915+105) and thus its fate is uncertain. In addition, Misra & Melia (1996) showed that in the context of the two-temperature model, there should also be a rather extended transition region between the hot source and the cold outer disk. The requirement of the existence of such a transition region in GRS 1915+105 appears to contradict the results of Belloni et al. (1997a,b), who were able to fit the source spectra reasonably well with a simple multi-color disk blackbody model using a rather small R_{in} .

Taam et al. (1997) and Chen et al. (1997) argued that the geometry of the disk in GRS 1915+105 is that of a cold outer disk extending from some $r_{\text{in}} \sim 30$ to infinity, plus a hot, optically thin inner region between $r = 3$ and r_{in} . They interpreted the spectral changes from hard/lower luminosity states to softer/higher luminosity states as arising from a decrease in the value of r_{in} . The inner disk region was not modeled by these authors, and instead it was assumed that its behavior is simply modulated by the changes in the accretion rate through the outer disk. But let us now consider this suggestion in more detail. Suppose that when the accretion rate increases, the inner region shrinks in size from r_c to $r_h < r_c$. Since the spectral index changes considerably from the cold to the hot state, $r_c - r_h \sim r_c$, i.e., the inner disk radius should decrease substantially (as an illustration of our point, see Poutanen, Krolik, & Ryde 1997 for the case of spectral transitions in Cyg X-1, where it is found that $r_c \simeq 40$ and $r_h \simeq 8$). The region $r_h < r < r_c$ should cool to the temperature and height appropriate for the Shakura-Sunyaev disk. To be applicable to GRS 1915+105, this cooling must happen on a thermal time scale. Thus, $\Sigma \sim \Sigma_0$, where $\Sigma_0 \lesssim$ few is the hot inner disk column density. Let us now estimate the accretion rate through this region immediately after a transition takes place. The accretion rate is given

by $2\pi R \Sigma v_R$, and it is only v_R in this expression that can change on a thermal time scale. From Equation (6) we have $v_R \sim 3\alpha c r^{-1/2} (H/R)^2$. The ratio of the accretion rate in the high state, \dot{M}_h , to that in the cold state, \dot{M}_c , is

$$\frac{\dot{M}_h}{\dot{M}_c} = \left(\frac{H_{\text{cold}}}{H_{\text{hot}}} \right)^2 \sim \left(\frac{H_{\text{cold}}}{R} \right)^2 \sim 10^{-3}, \quad (\text{A1})$$

where a value of $H_{\text{cold}}/R \sim 0.03$ is used, since this is when the radiation to gas-pressure transitions happen in the standard accretion disk theory for $M_1 \sim 1$ (e.g., SZ94). The inner hot region is starved and its luminosity is correspondingly lower (by a factor of 10^3 if there is no advection, or by a factor of 10^6 if advection is important, since in the latter case the efficiency of conversion of the accretion power into radiation decreases proportionally to the decrease in \dot{M}). Furthermore, the luminosity of the torus $r_h < r < r_c$ also decreases in the same proportion, because the local flux from the disk is $F_d = 3GM\dot{M}/8\pi R^3 \propto \dot{M}$. We conclude that if the radius of the hot inner region suddenly increases, then the *luminosity of the system should first significantly decrease before it goes up*.

The time necessary for the inner disk to recover from this and become brighter than it was in the cold (hard) state is simply given by the filling time of the transition region. This time is $t_r \sim (R_c - R_h)/\nu \sim R_c/\nu \equiv t_v(R_c)$, where $t_v(R_c)$ is the viscous time at R_c . The disk instability itself in the Taam et al. (1997) picture happens at a yet larger radius. However, the results of Belloni et al. (1997a,b) show that this radius cannot be much larger than r_c . In that case, we have just shown that the cold to hot transition in the framework of a central varying source should first have a dip in luminosity and a slower recovering phase, with the rise time comparable to that of the whole instability cycle. It is also worthwhile mentioning that following this reasoning, a transition from the hot to the cold state would first produce a strong flare. The problem here is that one needs to dispose of the transition region mass during a thermal time scale in order to extend the hot region from r_h to r_c , which means that during that time the accretion rate exceeds the average accretion rate by approximately $(R/H_c)^2 \sim 10^3$. Needless to say, neither substantial dips nor bright flare-ups are observed in GRS 1915+105 at the end of the hot state, and for this reason we believe that the geometry of a central source with a varying radius is inconsistent with the observations.

In addition, it is questionable whether the boundary conditions used by Abramowicz et al. (1995) at the interface between the cold and hot portions of the disk (i.e., $dT/dR = 0$ and $d\Sigma/dR = 0$) are justifiable, because at this point one would expect these gradients to be the largest in the disk. It appears to us that more appropriate boundary conditions would be given by the continuity of mass flow at $r = r_c$, i.e., $d\dot{M}/dr = 0$, and continuity in the radial energy flux, or specifying a temperature gradient at this point, $dT/dr = -(T_{\text{in}} - T_c)/\delta l$, where T_{in} is the inner disk temperature and δl is a characteristic scale of the “boundary layer” between the two disk segments. Of course, a completely self-consistent solution would only be obtained when one also includes the time-dependent inner disk equations and solves the whole disk evolution through the instability.

Concluding this section, we believe that the geometry of a hot central source plus a cold disk with a variable interface between the two is not appropriate for GRS 1915+105, and that one needs to do a careful study to see whether this model can be applied to any time-dependent phenomena in GBHCs or LMXBs. Further, a central source with a fixed boundary is not ruled out by our considerations here, but then the main attraction of the model – the simple picture of spectral hardening or softening as being due to change in r_{in} – no longer exists.

Cold Disk Plus a Hot Overlying Corona

A geometry that satisfies the constraints $H/R \lesssim 0.1$ is that of a geometrically thin and cold (compared with an ADAF, for example) accretion disk with a hot, optically thin corona above it. The accretion disk height scale H is reduced from the value given by the Shakura-Sunyaev theory due to the additional coronal cooling by the factor $1 - f$ (see Equation 7 in Svensson & Zdziarski 1994). In this picture, the thermal disk emission corresponds to the multi-temperature blackbody emission modeled by Belloni et al. (1997a,b) and Muno et al. (1999), whereas the non-thermal power-law is generated within the corona. The corona itself may be localized, consisting of magnetic flares (e.g., Haardt, Maraschi & Ghisellini 1994; Nayakshin 1998) or it may be extended, with a vertical scale anywhere between H and the local disk radius. This latter possibility does not contradict our previous estimates of $t_{\text{th}}/t_{\text{visc}}$, since it is the cold disk below the corona wherein most of the mass is contained, and thus it is the scale height of the cold disk that defines $t_{\text{visc}}/t_{\text{visc}}$.

B. EFFECTS OF THE ENHANCED ENERGY TRANSPORT

Throughout our studies, we deliberately used the fraction f in the cooling term in the energy balance equation (eq. 5), rather than in the heating term, as was done by Abramowicz et al. (1995) and Taam, Chen & Swank (1997). The latter approach assumes that the energy released in the disk is reduced by the factor $(1 - f)$, i.e., a fraction $(1 - f)$ of the viscously released energy was not even deposited in the disk, and that the cooling rate is the same as in the standard model. In our approach, all the energy is released in the disk, and it is the energy transport out of the disk that is being increased rather than the heating being decreased. We believe that our formulation of the problem follows what physically occurs in a disk-corona system. In static accretion disk models, wherein one can neglect radial energy transport, both formulations will give identical results, since only the two first terms on the right hand side of Equation (5) are non zero. However, in a time dependent situation, moving the factor $(1 - f)$ from the cooling term to the heating term results in an unphysical re-normalization of these two terms relative to the other terms of Equation (5), and thus may give rise to a serious error.

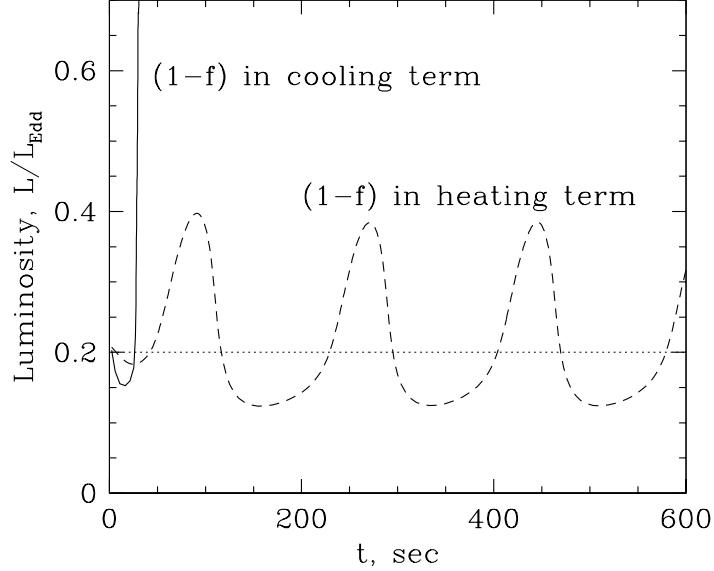


FIG. B12.— Instabilities of the standard accretion disk theory with the coronal cooling included in the (i): cooling term, as is done in this paper (solid line); (ii) heating term, which is unphysical (dashed line). Note that the first model would actually saturate at a very high luminosity, but the resulting pattern of outbursts would consist of a series of spikes or sharp bursts, and would never be able to reproduce variability such as that seen in panel (c) of Figure 1 for GRS 1915+105. The model parameters used to generate this figure are: $\dot{m} = 0.2$, $f = 0.75$, and $M = 10 M_{\odot}$.

We have run our disk evolution code for different values of the accretion rate \dot{m} and the fraction f to determine whether a supplemental vertical energy transport added to the standard Shakura-Sunyaev disks with constant α can explain the observations of GRS1915. All of our models with accretion rates sufficiently high to produce radiation pressure dominated regions over a portion of the standard disk were found to be unstable. Moreover, none of the simulated bolometric light curves became saturated, i.e., all the models ran away to arbitrarily high temperatures and low optical depths. Physically, this means, of course, that we would need to modify our code to include the optically thin case; this would presumably lead to a saturation in the instability, followed by a gradual decline in the luminosity and a return to the gas-dominated quasi-stable state. However, such oscillations would be fundamentally different than the ones observed in GRS 1915+105. In particular, the standard disk (with $\alpha = \text{const}$) plus corona system would produce quasi-periodic spike-like outbursts, with a very large ratio of maximum to minimum luminosity, and a very small duty cycle (see, e.g., Cannizzo 1996, 1997), whereas GRS 1915+105 displays a variety of behaviors, many of which have duty cycles larger than a half. Thus, we conclude that the standard viscosity law, even with the addition of a corona cannot explain the observations of GRS 1915+105.

On the other hand, Abramowicz et al. (1995), and Taam et al. (1997) found a mild oscillatory behavior for a range of \dot{m} and f . We believe that the disagreement is entirely due to the difference discussed above in the treatment of the effects of the corona above the disk. To check this, we placed the *cooling* term due to the additional energy transfer from the disk to the corona, into the heating term, as was done by these authors, and ran several tests. With this, we were indeed able to reproduce their results. In Figure (B12), we show the difference in the resulting light curves that the positioning of the coronal cooling term makes. The solid curve shows the results of our code with f placed in the cooling term, as explained above. In contrast, the dashed curve shows the light curve with the coronal cooling placed in the heating term. It can be seen that the instability indeed saturates when one uses the latter (unphysical) formulation of the problem, and oscillations with a reasonable amplitude follow.

In all of these calculations, we have assumed that the fraction of power transmitted by the additional energy transfer mechanism is a constant independent of the local conditions in the disk. However, the spectrum of GRS 1915+105 in the high state is generally (but not always) softer than it is in the low state (e.g., Belloni et al. 1997a,b; Munoz et al. 1999), so that f probably decreases from the low to the high state. One then might wonder whether allowing f to vary in accordance with the observations would change our conclusions and allow the standard accretion disk theory to reproduce the observed instabilities in GRS 1915+105. Unfortunately, this effect actually goes the wrong way, making the instability stronger. The presence of the corona always decreases the extent of the unstable region in the disk (e.g., Svensson & Zdziarski 1994). In order to suppress the runaway process illustrated by the solid curve in Fig. (B12), one would need the fraction f to be larger in the high state than it is in the low state, which is opposite to what is observed. Summarizing, we discount the notion that a hot corona is sufficient to make the disk unstable in the correct manner to explain the observations. The standard accretion disk with a standard viscosity prescription, with or without a corona, is unstable in the radiation-dominated regime and yields a burst-like behavior that is incompatible with the observations of GRS 1915+105.

REFERENCES

Abramowicz, M.A., et al. 1988, *ApJ*, **332**, 646.

Abramowicz, M.A., Chen, X., & Taam, R. 1995, *ApJ*, **452**, 379.

Bailyn, C.D., Orosz, J.A., McClintock, J.E., & Remillard, R.A. 1995, *Nature*, **378**, 157.

Barret, D., McClintock, J.E., & Grindlay, J.E. 1996, *ApJ*, **473**, 963.

Bath, G.T., & Pringle, J.E. 1982, *MNRAS*, **199**, 267.

Belloni, T. et al. 1997a, *ApJL*, **479**, L145.

Belloni, T. et al. 1997b, *ApJL*, **488**, L109.

Bisnovatiy-Kogan, G.S., & Lovelace, R.V.E. 1997, *ApJL*, **486**, L43.

Bisnovatiy-Kogan, G.S., & Blinnikov, S.I. 1977, *A&A*, **59**, 111

Cannizzo, J.K. 1993, *ApJ*, **429**, 318.

Cannizzo, J.K., Chen, W., & Livio, M. 1995, *ApJ*, **454**, 880.

Cannizzo, J.K. 1996, *ApJL*, **466**, L33.

Cannizzo, J.K. 1997, *ApJ*, **482**, 178.

Castro-Tirado, A.J., Brandt, S., & Lund, S. 1992, IAU Circ, 5590

Chen, X., & Taam, R.E. 1993, *ApJ*, **412**, 254.

Chen, X., & Taam, R.E. 1994, *ApJ*, **431**, 732.

Chen, X., Swank, J.H., & Taam, R.E. 1997, *ApJL*, **477**, L41.

Eikenberry, S.S. et al. 1998, *ApJL*, **494**, L61.

Fender, R.P., & Pooley, G.G. 1998, *MNRAS*, **300**, 573.

Frank, J., King, A., & Raine, D. 1992, Accretion Power in Astrophysics (Cambridge, UK: Cambridge University press)

Gliozzi, M., Bodo, G., & Ghisellini, G. 1999, *MNRAS*, **303**, L37.

Goldman, I., & Wandel, A. 1995, *ApJ*, **483**, 187.

Greiner, J., Morgan, E., & Remillard, R.A. 1996, *ApJL*, **ApJ**, 473.L107

Haardt, F., & Maraschi, L. 1991, *ApJL*, **380**, L51.

Haardt, F., Maraschi, L., & Ghisellini, G. 1994, *ApJ*, **432**, L95.

Lightman, A.P., & Eardley, D.M. 1974, *ApJL*, **187**, L1.

Magdziarz, P., & Zdziarski, A.A. 1995, *MNRAS*, **273**, 837.

Menou, K., Hameury, J.-M., Stehle, R. 1998, preprint

Meyer, F. 1984, *A&A*, **131**, 303

Meyer, F., & Meyer-Hofmeister, E. 1981, *A&A*, **104**, L10

Mirabel, I.F., & Rodrigues, L.E. 1994, *Nature*, **371**, 46.

Mirabel, I.F. et al. 1997, *A&A*, **330**, L9

Misra, R., & Melia, F. 1996, *ApJ*, **467**, 405.

Morgan, E., Remillard, R.A., & Greiner, J. 1997, *ApJ*, **482**, 993.

Muno, M.P., Morgan, E.H., & Remillard, R.A. 1999, submitted to *ApJ*, astro-ph/9904087

Narayan, R., & Yi, I. 1995, *ApJ*, **452**, 710.

Nayakshin, S., & Melia, F. 1997, *ApJL*, **490**, L13.

Nayakshin, S. 1998, PhD thesis, University of Arizona (astro-ph 9811061).

Nayakshin, S., & Dove, J.B. 1999, submitted to *ApJ* (astro-ph 9811059).

Poutanen, J., Krolik, J.H., & Ryde F. 1997, *MNRAS*, **292**, L21.

Sakimoto, P.J., & Coronitti, F.V. 1989, *ApJ*, **342**, 49.

Shakura, N.I., & Sunyaev, R.A. 1973, *A&A*, **24**, 337

Shapiro, L.E., Lightman, A.P., & Eardley, D.M. 1976, *ApJ*, **204**, 187.

Stella, L., & Rosner, R. 1984, *ApJ*, **277**, 312.

Svensson, R., & Zdziarski, A. A. 1994, *ApJ*, **436**, 599.

Szuszkiewicz, E., Malkan, M.A. & Abramowicz, M.A. 1996, *ApJ*, **458**, 474.

Szuszkiewicz, E., & Miller, J.C. 1998, *MNRAS*, **298**, 888.

Taam, R.E., & Lin, D.C. 1984, *ApJ*, **287**, 761.

Taam, R., Chen, X., & Swank, J.H. 1997, *ApJL*, **485**, L83.

Vishniac, E.T., & Wheeler, J.C. 1996, *ApJ*, **471**, 921.

Zhang, S.N., et al., 1994, IAU Circ., 6046